A response surface methodology for optimization of 2,4-dichlorophenoxyacetic acid removal from synthetic and drainage water: a comparative study

Mohammad Javad Amiri *[1], Mehdi Bahrami [1], Bahare Beigzadeh [1] and Antonio Gil [2]

[1] Department of Water Engineering, College of Agriculture, Fasa University 74617-81189, Fasa, Iran.

[2] INAMAT-Department of Sciences, Public University of Navarra, Campus of Arrosadia, 31006 Pamplona, Spain.

***** Corresponding author: Email: mj_amiri@fasau.ac.ir, Tel.: +989173157688, Fax: +987313340519.

Abstract

The potential of a granular activated carbon (GAC), a rice husk biochar (BRH) and multi-walled carbon nanotubes (MWCNTs) for removing 2,4-dichlorophenoxyacetic acid (2,4-D) from simulated wastewater and drainage water has been evaluated. In this regard, a response surface methodology (RSM) with a central composite design (CCD) (CCD-RSM design) was used to optimize the removal of 2,4-D from simulated wastewater under different operational parameters. The maximum adsorption capacities followed the order GAC > BRH > MWCNTs, whereas the equilibrium time increased in the order MWCNTs < GAC < BRH. In the case of GAC and BRH, the 2,4-D removal percentage increased significantly upon increasing the adsorbent dosage and temperature and decreased upon increasing the initial 2,4-D concentration and pH. The results showed that the contact time and temperature were not important as regards the adsorption efficiency of 2,4-D by MWCNTs, whereas rapid removal of 2,4-D from simulated wastewater was achieved within the first 5 min of contact with the MWCNTs. The results confirmed that the Freundlich isotherm model with the highest coefficient of determination (R^2) and the lowest standard error of the estimate (SEE) satisfactorily fitted the 2,4-D experimental data. In addition, successful usage of the three adsorbents investigated was observed for removal of 2,4-D from drainage water from an agricultural drainage system. An economic analysis with a rate of return (ROR) method indicated that BRH could be used as an eco-friendly, low-cost, versatile and high adsorption capacity alternative to GAC and MWCNTs for the removal of 2,4-D.

Keywords: 2,4-dichlorophenoxyacetic acid adsorption, Central composite design, Response surface methodology, drainage water, Rate of return method.

Introduction

The high consumption of pesticides and herbicides to increase agricultural production is a major environmental and health problem in all parts of the world, and particularly in Iran (Ebrahimizadeh et al. 2009). The extensive use of herbicides by farmers can easily contaminate surface water and groundwater, which may have harmful effects on human health. As such, it is important to prevent the release of these compounds into the environment due to their high mobility (Bakouri et al. 2008).

2,4-Dichlorophenoxyacetic acid (2,4-D) is an ionizable herbicide from the phenoxyacetic acid family that is potentially hazardous for surface water bodies and groundwater aquifers (Boivin et al. 2005; Salmon and Hameed 2010). 2,4-D is commonly used to control broad-leaf weeds and grass in wheat, maize, oat, rye and cane crops due to its good selectivity and low cost (Aksu and Kabaskal 2005; Salmon and Hameed 2010). The half-life of 2,4-D, which is applied at between 50 and 100 L ha^{-1} in aerobic and anaerobic aquatic environments, has been estimated to be 15 days and 41-333 days (Aksu and Kabaskal 2004;. Liang et al. 2015). The maximum contaminant level of 2,4-D for drinking water and irrigation is 70 and 100 ppb according to the U.S. Environmental Protection Agency (2015).

Various methods, including ion-exchange (Humbert et al. 2008), advanced oxidation (Saritha et al. 2007), membrane technologies (Ahmad et al. 2008), biological treatment (Santacruz et al. 2005) and adsorption (Bazrafshan et al. 2013; Dehghani et al. 2014; Abigail and Chidambaram 2016), have been used to remove 2,4-D from contaminated waters. Of these various water purification and recycling technologies, adsorption is a fast, inexpensive and universal method (Arshadi et al. 2014). Indeed, the use of adsorbents such as activated carbons (Aksu and Kabaskal 2004 and 2005; Hameed et al. 2009; Salmon and Hameed 2010) and ion-exchange resins (Ding et al. 2012) for removal of 2,4-D is common. As such, the search for efficient and inexpensive materials instead of commercial adsorbents to eliminate 2,4-D from

surface and groundwater is ongoing. Many researchers have turned their interest toward cheaper adsorbents such as silica gel (Han et al. 2010), clay minerals (de Rezende et al. 2011), char prepared from corncobs, bamboo and wood chips (Kearns et al. 2014), rice husk ash (Deokar and Mandavgane 2015), modified jute (manna et al. 2016), rice husk nanosorbents (Abigail and Chidambaram 2016), and biochar generated from bamboo, oak wood and tea waste (Mandal et al. 2017). Although these adsorbents have a remarkable potential for 2,4-D removal, but most of these materials work well only under acidic pH range and the application of them for various experimental conditions is questionable.

In the last decade, rice husk has been employed as a versatile material for removal of a wide range of pollutants, such as heavy metals (Srivastava et al. 2006), dyes (Ahmaruzzaman and Gupta 2011) and other compounds (Imagawa et al. 2000; Abigail and Chidambaram 2016), due to its eco-friendly nature, ready availability and low cost. Rice husk comprises 75% organic compounds and 15% silica by weight (Abigail and Chidambaram 2016) and the annual production of rice husk in Iran is about 500,000 tons (Rostamian et al. 2015). However, although it can be used as a filter for wastewater treatment systems, there is no large-scale procedure for rice husk usage in Iran. Recent advances in nanotechnology have also led to the development of novel nanomaterials, which provide a remarkable potential in water and wastewater treatment. Nanomaterials such as ferric oxide (Fe_3O_4), titanium oxide (TiO_2), manganese oxide (MnO_2), nano zero valen iron (nZVI) and carbon nanotubes (CNTs) can be defined as materials smaller than 100 nm in at least one dimension (Qu et al. 2013). Classification of nanomaterials is based on the number of dimensions as below: (1) zero-dimensional (0-D), wherein all the dimensions are at nanoscale such as fullerenes; (2) one-dimensional (1-D), wherein two dimensions are at nanoscale such as nanotubes and nanorods; (3) two-dimensional (2-D), wherein one dimension is at nanoscale such as nanofilms; (4) three-dimensional (3-D), wherein all the dimensions are not at nanoscale such as graphite. Moreover,

nanomaterials can be classified into four types: carbon based materials, metal based materials, dendrimers and composites. The unique properties of these various types of nanomaterials have been proposed for potential applications in commercial, medical, military, and environmental sectors. Among these materials, carbon nanotubes due to its high specific surface area, tunable surface chemistry and easy reuse have been broadly used in environmental remediation (Qu et al. 2013)

In the present work, the performance and effectiveness of three adsorbents, including a granular activated carbon (GAC), a rice husk biochar (BRH) and multiwall carbon nanotubes (MWCNTs), for the removal of 2,4-D from synthetic and drainage water was evaluated and compared. Biochar is a carbon-rich porous substance synthesized by pyrolysis of organic compounds (Kearns et al. 2014), and GAC has shown great potential for the removal of various organic (Shirmardi et al. 2016) and inorganic (Edvin Vasu 2008) pollutants due to its characteristic microporous structure, high adsorption capacity and large specific surface area. Biochars with active functional groups, high porosity and a large surface area have been widely applied to eliminate several pollutants, such as organic compounds (Hallin et al. 2017) pesticides (Kearns et al. 2014) and heavy metals (Wang and Liu 2017). More recently, MWCNTs have attracted increasing attention due to their inimitable structure and excellent properties (Bahrami et al. 2017a). Indeed, these materials have been favorably employed for the elimination of pollutants such as caffeine (Bahrami et al. 2017a), pigments (Ehyaee et al. 2017), heavy metals (Iannazzo et al. 2017) and pharmaceuticals products (Wang et al. 2016), amongst others.

The optimization of operational parameters such as pH, temperature (T), contact time (t), adsorbent dose (C_s) and initial herbicide concentration (C_0) is necessary in order to decrease the number of tests and determine the optimum conditions for input variables. In this regard, the response surface methodology (RSM) coupled with central composite design (CCD) (CCD-

RSM design) is an efficient tool that has been used to model the correlation between output response and input of the machining process (Ehyaee et al. 2017; Mourabet et al. 2017). RSM is a combination of numerical optimization techniques and statistical design that has been used to optimize processes and product designs (Ehyaee et al. 2017; Mourabet et al. 2017).

To the best of our knowledge, no attention has been paid to comparing the adsorption capacity of biochar, GAC and MWCNTs for the removal of 2,4-D from synthetic and drainage water using RSM. Thus, the main goals of this work were: (i) to evaluate the adsorption capacity of GAC, BRH and MWCNTs for removal of 2.4-D from synthetic and drainage waters; (ii) to optimize the effect of input parameters on the adsorption processes and to reduce the number of tests by RSM; (iii) to compare the evaluation of economic aspects for GAC, BRH and MWCNTs using the Rate of Return (ROR) method; and (iv) to investigate the equilibrium isotherm models to determine the possible mechanism of herbicide adsorption. This study showed BRH to be a cheap and sustainable material that could be a viable alternative to GAC and MWCNTs for remediation and treatment scenarios, particularly in developing countries.

Experimental

Adsorbents

GAC and MWCNTs were purchased from Merck (Germany), whereas rice husk (RH) biochar was produced according to the following procedure (Rostamian et al. 2015). RH was washed with boiling distilled water and dried for 24 h at 105 °C. The material obtained was then crushed and passed through sieves of various sizes until an average particle size of less than 5 µm had been achieved. The resulting RH powder was carbonized under purified nitrogen (99.9%), heating from 25 °C to 800 °C at a heating rate of 10 °C min^{-1}, then maintained at 800 °C for 2

h. This substance is referred to as BRH. Some of the important physical characteristics of the adsorbents used are given in Table 1.

Chemicals

Analytical grade 97.5% pure 2,4-D from Sigma Aldrich Co. was applied as an adsorbate with no further purification. The chemical structure and physicochemical properties of 2,4-D are presented in Table 2 (Hameed et al. 2009). 2,4-D at a concentration of 1000 mg L^{-1} was employed as a stock solution, and the various concentrations were obtained by diluting this stock solution with deionized water.

Batch adsorption studies

Adsorption experiments were performed by adding various amounts of BRH, GAC and MWCNTs (0.05-0.2 g) to several 2,4-D concentrations (2-800 mg L^{-1}) at an initial pH of between 2 and 9, and at various temperatures (20-60 °C) and contact times (0-120 min). The flasks were then shaken at 130 rpm and the mixtures filtered using Whatman 42 filter paper. Finally, the concentration of 2,4-D in the solution was determined by UV-Vis spectrophotometry (Shimadzu UV/vis 2100, Japan) at 283 nm. The calibration curve was plotted using the spectra for the standard solutions. The adsorption capacities of BRH, GAC and MWCNTs (mg g^{-1}) under equilibrium conditions (q_e, mg· g^{-1}) and the adsorption efficiency (E, %) were determined using the following equations:

$$q_e = \frac{(C_0 - C_e)}{m} V \quad (1)$$

$$E = \frac{(C_0 - C_e)}{C_0} \times 100 \quad (2)$$

where C_e and C_0 (mg L^{-1}) are the equilibrium and initial liquid-phase concentrations of 2,4-D, V (L) is the volume of the solution, m (g) is mass of the dry adsorbents, and q_e and E are the 2,4-D uptake at equilibrium and the removal efficiency of 2,4-D, respectively.

RSM

RSM includes a collection of statistical and mathematical methods that are employed to optimize and analyze the interaction between factors under various conditions and thereby delimit the experimental studies of the processes. In this regard, CCD-RSM was designed using MINITAB version 16 software to model systems in which the adsorption efficiency of adsorbents is affected by multiple operational factors, including pH, temperature, contact time, adsorbent dose and initial herbicide concentration. A total of 54 tests were designed for each adsorbent to optimize the adsorption of 2,4-D. The ranges of the operational parameters are given in Table 3.

Rate of Return (ROR) method

The rate of return (ROR) on investment can be applied as a common method to determine the most cost-effective projects, with the acceptance or rejection thereof being based on a comparison between ROR and minimum attractive rate of return (MARR) indices. In brief, the project is considered economical if ROR is higher than MARR and the project is rejected if ROR is lower than MARR. An extra investment analysis was employed as a criterion to determine the status of two or more economical projects. The details of this procedure have been reported previously (Remer and Nieto 1995).

Mathematical isotherm adsorption models

Isotherm adsorption models were used to present the relationship between 2,4-D in solution and the amount of 2,4-D adsorbed on BRH, GAC and MWCNTs by contact at a fixed temperature. For isotherm studies, 0.1 g of BRH, GAC and MWCNTs was added to 100 mL

of 2,4-D solutions at concentrations in the range of 2 to 800 mg L^{-1} at the optimum pH for a contact time of 120 min. All mixtures were shaken at 130 rpm at room temperature. The Langmuir, Freundlich, Langmuir-Freundlich and Redlich-Peterson isotherm models (see Table 4) were applied to fit the experimental data of 2,4-D removal. The goodness of fit between the experimental data and isotherm model estimations was assessed using coefficient of determination (R^2) and standard error of estimate (SEE). R^2 and SEE are defined as:

$$R^2 = \frac{\sum_{i=1}^{n}\left[\left[(q_e)_{pre} - (\overline{q_e})_{pre}\right]\left[(q_e)_{\exp} - (q_e)_{\exp}\right]\right]}{\sum_{i=1}^{n}[(q_e)_{\exp} - (\overline{q_e})_{\exp}]^2 \sum_{i=1}^{n}\left[(q_e)_{pre} - (\overline{q_e})_{pre}\right]^2} \quad (3)$$

$$SEE = 1 - \left[\frac{\sum_{i=1}^{n}[(q_e)_{pre} - (q_e)_{\exp}]^2}{n-2}\right]^{0.5} \quad (4)$$

where $(q_e)_{exp}$ and $(q_e)_{pre}$ are the observed and estimated data, respectively. $(\overline{q_e})_{\exp}$ and $(\overline{q_e})_{pre}$ are the average of the observed and experimental data, respectively, and *n* is the data numbers. As the value of R^2 is closer to 1.0 and the value of SEE is closer to 0.0 the accuracy of model is higher.

Characterization techniques

Solution pH measurements were performed using dilute HCl and NaOH solutions and a pH-meter (Hach senseion3, USA). The pore-size distribution and specific surface area of BRH, GAC and MWCNTs were characterized using the Barret, Joyner and Halenda (BJH) and Brunauer–Emmett–Teller (BET) methods. The pore structure and surface morphology of the adsorbents were observed by scanning electron microscope (SEM) using a TESCAN-Vega 3 instrument. Infrared wave numbers (cm^{-1}) for the adsorbents were recorded using KBr pellets on a Jasco FT/IR-680 plus spectrophotometer. The solid addition method was employed to

determine the point of zero charge (pH_{PZC}) (Rostamian et al. 2015). The concentration of 2,4-D in drainage water was measured by HPLC (Shimadzu UFLC-2010, Japan) on a C_{18} column with a length of 250 mm and an internal diameter of 4.6 mm. The column was calibrated and the coefficient of determination (R^2) for the calibration curve found to be 0.999. A 70/30 (v/v) mixture of acetonitrile and water was used as the mobile phase. A diode array PDA detector operating at a wavelength of 284 nm was used to detect 2,4-D.

Drainage water

The effectiveness and performance of the three adsorbents studied were also investigated for the adsorption of 2,4-D from drainage water obtained from an agricultural drainage system, which contained total dissolved solids (TDS) of 3809 mg L^{-1} and was filtered using a 0.45 µm filter membrane. The effect of co-existing cations and anions was also investigated by assessing the interference effect of K^+, Na^+, Ca^{2+}, Mg^{2+}, Cl^-, HCO_3^- and SO_4^{2-}. These ions were chosen because they were present in drainage water. The characteristics of the drainage water used are summarized in Table 5.

Results and discussion

Selection of the adsorbents

A wide range of adsorbents was initially tested for the removal of 2,4-D from contaminated water (see Table 6). However, none of them provided favorable results or a good ability to remove 2,4-D. Previous studies indicated that the removal of 2,4-D from wastewater is more difficult than for other organic pollutants (Kearns et al. 2014), which can be explained by the fact that 2,4-D is a polar molecule with an ionization constant (pKa) of 2.64 that exhibits high water solubility. Finally, BRH, GAC and MWCNTs were used to adsorb the herbicide from

synthetic and drainage water and a comparative study of these adsorbents was performed in terms of adsorption capacity, optimum time of adsorption and economic analysis.

Characterization of BRH, GAC and MWCNTs

As can be seen from the data included in Table 1, the average pore sizes of GAC, BRH and MWCNTs were 4.2, 5.9 and 7.2 nm, respectively, thus showing that the pore structure of the three adsorbents was in the range 2 to 50 nm and was therefore a mesoporous structure (Zeng et al. 2018). The higher average pore diameter for MWCNTs compared with other adsorbents facilitates mass transfer between the surface of the adsorbent and 2,4-D in solution (Amiri et al. 2016; Bahrami et al. 2017a). The specific surface area of GAC was 728 m^2 g^{-1}, which is about 2.3- and 3.64-times higher than that for BRH (320 m^2 g^{-1}) and MWCNTs (200 m^2 g^{-1}), respectively. The larger specific surface area of GAC leads to a greater accessibility to active sites in contact with 2,4-D in solution. The pore volume of GAC was 0.748 cm^3 g^{-1}, compared to 0.431 and 0.348 cm^3 g^{-1} for BRH and MWCNTs, respectively. As such, the trend in variation in pore volume is similar to that for the total surface area.

Changes in the pore structure and surface morphology of BRH, GAC and MWCNTs after 2,4-D adsorption were examined by SEM. BRH is a black powder synthesized by pyrolysis of rice husk under an oxygen-depleted atmosphere (see Fig. 1(A)). GAC has a larger particle size than BRH and MWCNTs and therefore can easily be used in water-treatment systems (see Fig. 1(B)). MWCNTs are highly versatile materials that are available as black powders (see Fig. 1(C)). The SEM micrograph for BRH is shown in Figure 1(D). It can be seen that the carbonization temperature required for chemical activation of rice husk resulted in a change to the surface of the precursor and the formation of different pore shapes and sizes. The surface of GAC exhibited roughness, including heterogeneous cavities and coarse and well-distributed pores for 2,4-D adsorption (see Fig. 1(F)). The morphology of BRH and GAC was not obviously changed after 2,4-D adsorption (see Fig. 1(E) and Fig. 1(G), respectively). Inspection

of the SEM images (see Fig. 1(H)) clearly shows MWCNTs with a well-developed porous structure. However, post-treatment, the surface of MWCNTs is coated with a thin layer of 2,4-D (see Fig. 1(I)). Moreover, the carbon chain of MWCNTs has changed and it can be seen that 2,4-D adsorption significantly affects the surface morphology.

The surface functional groups on BRH, GAC and MWCNTs were identified before and after 2,4-D adsorption by FT-IR spectroscopic analysis in the range 400-4000 cm^{-1} (see Fig. 2). The results indicated that the FT-IR spectra of BRH, GAC and MWCNTs are very similar to each other. The intensity of functional groups for BRH was greater than that for GAC and MWCNTs. The broad peak at about 3400-3500 cm^{-1} for GAC corresponds to hydroxyl groups (O-H) in phenols, carboxylic acids and alcohols (see Fig. 2A), whereas the weak peak at about 2800-3000 cm^{-1} is assigned to the C-H stretching vibration in the alkane group (see Fig. 2A). The band at 2345 cm^{-1} is associated with C≡C stretching vibrations in alkyne groups (Anisuzzaman et al. 2015), and the peak at 1509 cm^{-1} is associated with C=C stretching vibration in the aromatic C-C bond (Al-Qodah and Shawabkah 2009). The small peaks between 1300-1800 cm^{-1} can be assigned to carbonyl groups (C=O) in carboxylic, ketone, lactone and aldehyde groups (Anisuzzaman et al. 2015) (see Fig. 2A), and the strong peaks in the range 1300-1800 cm^{-1} are due to C-O-C stretching vibration in phenols, alcohols, esters and ethers (Al-Qodah and Shawabkah 2009; Anisuzzaman et al. 2015) (see Fig. 2A). The bands at around 1033 cm^{-1} are assigned to C–H in plane absorptions (Mohammad and Ahmed 2017). In the case of BRH, the peaks at about 3400-3500 cm^{-1} are due to the phenolic O–H stretching band, whereas the peaks at about 2800-3000 cm^{-1} are related to $-CH_2$ and $-CH_3$ stretching bands (Chen et al. 2011). The peak at 1577 cm^{-1} is due to the aromatic C=C stretching vibration (Chen et al. 2011) and the strong absorption peak at 1041 cm^{-1} is assigned to Si-O-Si stretching bands (Rostamian et al. 2015). In the case of MWCNTs, the absorption peak at 3444 cm^{-1} could be related to O-H bonds associated with hydroxyl groups and several peaks at about 2800-3000

cm^{-1} may be due to CHx groups (Leman et al. 2011). The peak at 1739 cm^{-1} corresponds to COOH groups, whereas the C=C stretching mode of MWCNTs was observed at 1635 cm^{-1} (Bahrami et al. 2017b). In addition, the peak at around 1273 cm^{-1} is due to the C–O stretching band (Arasteh et al. 2010). The peak shapes in the FT-IR spectrum of the adsorbents were significantly changed after 2,4-D adsorption. This could be attributed to the formation of new oxygen-containing groups on the surface, which have a marked influence on the surface adsorbent properties and adsorption characteristics (see Fig. 2B). The hydrophilic properties of GAC were considerably enhanced by these oxygen functional groups, which can act as binding sites for the removal of 2,4-D (Mohammad and Ahmed 2017). However, the spectrum of GAC displays a considerable shift in the -OH group from 3424 to 3458 cm^{-1}, along with a marked shift from 1041 to 1106 cm^{-1} that may be related to the electron-donating electrostatic interaction between the positive surface of GAC and the 2,4-D molecule (see Fig. 2B). The small peak at 1421 cm^{-1} observed in the spectrum of GAC (see Fig. 2A) is replaced by a broad band at 1438 cm^{-1} upon treatment of GAC with 2,4-D solution (see Fig. 2B). The new peaks at 538 and 876 cm^{-1} for the GAC surface are assigned to the 2,4-D molecule (see Fig. 2B). The presence of new peaks between 300-800 cm^{-1} in the spectra for BRH suggests a large quantity of 2,4-D molecules adhered to the surface of the adsorbent (see Fig. 2B). After adsorption of 2,4-D by BRH, a shift in the phenolic O–H stretching band from 3424 to 3436 cm^{-1} was detected. A shift in the peak for the aromatic C=C bonds in the spectra of BRH from 1577 to 1582 cm^{-1} was observed due to the appearance of a π-π interaction between 2,4-D and BRH (Zeng et al. 2018). Furthermore, the peak for the Si-O-Si stretching bands shifted from 1041 to 1092 cm^{-1} and new peaks were detected at 538, 3772 and 3922 cm^{-1} after adsorption of 2,4-D on the BRH surface (see Fig. 2B). After adsorption of 2,4-D by MWCNTs, the peaks for the -OH groups shifted from 3444 to 3450 cm^{-1}, the peaks for the CHx groups shifted from 2922 to 2914 cm^{-1}, the peaks for the COOH groups shifted from 1635 to 1630 cm^{-1} and the C–O

stretching bands shifted from 1273 to 1216 cm^{-1}. In addition, a new peak at 580 cm^{-1} in the spectra for MWCNTs shows the presence of 2,4-D molecules on the surface of the adsorbent.

The pH_{PZC} for BRH, GAC and MWCNTs was measured in 0.1 M KNO_3 solution in an initial pH range of between 1 and 12 (see Fig. 3). As can be seen from Figure 3, the pH_{PZC} curves for BRH, GAC and MWCNTs exhibit the same behavior, with values of 2, 4.1 and 8.3 for BRH, MWCNTs and GAC, respectively. At $pH < pH_{PZC}$, the net charge of the adsorbents is positive, while at $pH > pH_{PZC}$ the net charge of the adsorbents is negative. The surface of BRH has a lower pH_{PZC} in comparison with GAC and MWCNTs, thus demonstrating that their surface is negatively charged.

Optimization of 2,4-D adsorption using CCD-RSM

We have employed the CCD-RSM design to analyze and investigate the individual and interaction effects of the operational parameters and to determine the optimal conditions for 2,4-D adsorption by BRH, GAC and MWCNTs from simulated wastewater. The equilibration time and pH of the solution are two important factors affecting 2,4-D adsorption reactions. Thus, the initial solution pH affects the electrostatic interaction between the GAC, BRH and MWCNTs surface and 2,4-D (Aksu and Kabaskal 2004; Bazrafshan et al. 2013; Kearns et al. 2014). The interaction effects between pH and contact time when the other three factors were kept fixed are given in Figure 4. Generally, the adsorption efficiency of 2,4-D increased with increasing contact time and the equilibrium time for BRH and GAC was found to be 80 and 70 min, respectively (see Fig. 4A and 4B). However, it can be seen that the adsorption efficiency of 2,4-D by MWCNTs was not dependent on the contact time (see Fig. 4C). In this regard, it is important to note that MWCNTs removed 2,4-D with lower contact times due to their specific atomic structure. Indeed, the majority of 2,4-D (96%) was removed within the first 5 min of mixing with the MWCNTs. As can be seen from the results included in Figure 4, a pH value of less than 8.3 is suitable for the removal of 2,4-D from wastewater by GAC. This trend

can be attributed to the pH_{PZC} and the ionic nature of 2,4-D (Aksu and Kabaskal 2004). The surface of GAC will be positively charged at pH < 8.3 and negatively charged at pH > 8.3, whereas at pH < 4, 2,4-D preserves its molecular form and 78% of it will be in a neutral state (Ding et al. 2012). The large specific surface area of GAC (728 $m^2 g^{-1}$) is responsible for the adsorption of 2,4-D on the surface in this pH range (Ding et al. 2012). Moreover, the mobility of 2,4-D on the surface and subsurface of GAC is higher in an acidic medium (Al-Qodah and Shawabkah 2009). Indeed, at a pH of between 4 and 8, most 2,4-D is in an undissociated form, thus indicating that electrostatic attractions are not the predominant mechanism in this case. Due to the complex surface of GAC, which contains a significant number of functional groups, including phenolic, carboxyl, quinone and alcohol groups, as well as its water chemistry, several mechanisms are involved in the adsorption of 2,4-D in the pH range between 4 and 8. At pH > 8.3, 2,4-D is converted quickly to the anion form and the surface of GAC is negatively charged, thus resulting in electrostatic repulsion between the 2,4-D molecules and the negative charge on the GAC surface (Dehghani et al. 2014). As mentioned above, 2,4-D is a polar molecule which can be rapidly hydrolyzed at pH > 8. Previous studies have shown that the non-hydrolyzed molecule is favorably adsorbed on the surface of GAC (Al-Qodah and Shawabkah 2009). Therefore, the surface charge of GAC, speciation of 2,4-D and the degree of ionization are responsible for variations in the adsorption efficiency of 2,4-D in relation to pH. As such, the maximum adsorption efficiency of GAC was achieved at pH 2. Similar results concerning the effect of pH on the removal efficiency of 2,4-D by GAC in a batch system have been reported by Salmon and Hameed (2010). In the case of BRH, except when the pH is lower than 2, the surface of the adsorbent is negatively charged and becomes more negative with an increase in pH (see Fig. 3). Around pH 2, the neutral form of 2,4-D predominates and the surface of BRH is negative. However, the low adsorption efficiency of 2,4-D in this pH range shows that electrostatic interactions are not the dominant mechanism. Clearly, the adsorption

efficiency of 2,4-D by BRH increased dramatically in the pH range between 4 and 7 (see Fig. 4B) and the optimum pH was found to be 5.5. This phenomenon may be related to the formation of strong H-bonds between 2,4-D and phenolate or carboxylate functional groups on BRH (Zeng et al. 2018). At pH > 7, the competition between hydroxyl ions and the anion form of 2,4-D for binding to vacant BRH sites leads to a significant decrease in 2,4-D adsorption. In addition, an electrostatic repulsion between the anionic species of 2,4-D which can exist at pH > 7 and the negative charge of BRH may occur (Ding et al. 2012; Mandal et al. 2017). Thus, oxygen-containing groups, including phenolic hydroxyl, carbonyl and carboxyl, on the BRH surface are thought to be involved in the adsorption of 2,4-D molecules from simulated wastewater (Mandal et al. 2017). In the case of MWCNTs, it is well known that the maximum removal efficiency of 2,4-D is obtained at pH 2 and that the adsorption efficiency decreases significantly at higher pH (see Fig. 4C). Since 2,4-D is a polar molecule, π electron polarizability is a dominant mechanism in the adsorption process of 2,4-D (Li et al. 2011). As can be seen from the results presented in Figure 3, the surface of MWCNTs will be positively charged at pH < 4.1 and negatively charged at pH > 4.1. At pH < 3, 2,4-D remains in the non-ionized form and the surface of MWCNTs is positive. Under these conditions, the dispersion effect between the π-electrons of the MWCNTs and the aromatic phenolic ring is the predominant mechanism (Arasteh et al. 2010). At pH > 7, 2,4-D is dissociated and the anionic species of 2,4-D is formed. The degree of dissociation is markedly higher in the pH range 8-9. This process can be expressed as follows (Li et al. 2017):

$$2{,}4-D + OH^- \rightarrow 2{,}4-D^- \ (deprotonated\ form) + H_2O \qquad (5)$$

As such, an electrostatic repulsion between the deprotonated 2,4-D^- and the negatively charged MWCNTs occurs, thus resulting in a lower adsorption efficiency.

The interaction effects of reaction time and initial 2,4-D concentration when the other operational parameters were kept constant are shown in Fig. 5. The results show that the initial 2,4-D concentration plays an important role in achieving the maximum removal efficiency of 2,4-D. Thus, the removal efficiency of 2,4-D by GAC was more than 95% and became constant after 60-80 min, with an equilibration time of 70 min being achieved for GAC. A similar variation was observed in the case of BRH, with the adsorption efficiency increasing with increasing contact time and becoming constant after the equilibration time (80 min). At an initial concentration of 50 mg L^{-1}, the majority of 2,4-D (90%) was removed within the first minute of reaction with the MWCNTs. As mentioned before, the contact time is the least effective parameter in the 2,4-D adsorption process. These results also indicate that the adsorption efficiency of 2,4-D decreases with increasing initial 2,4-D concentration. In this regard, the highest 2,4-D removal efficiency was achieved at the lowest initial concentration (see Fig. 5) as numerous vacant sites are accessible on the adsorbent surface at low 2,4-D concentration. Upon increasing the initial 2,4-D concentration, the number of vacant adsorption sites decreases or they become saturated by herbicide molecules, therefore the residual sites are not readily accessible by 2,4-D molecules. This leads to a lower adsorption efficiency or a longer contact time to achieve the equilibrium adsorption rate.

The interaction effects of temperature and initial 2,4-D concentration for GAC, BRH and MWCNTs when the other operational parameters were kept constant are shown in Fig. 6. Clearly, the removal efficiency of 2,4-D decreases dramatically when increasing the initial pollutant concentration (see Fig. 6). Similarly, a sharp increase in 2,4-D removal percentage was found upon increasing the temperature from 20 to 46 °C for GAC and from 20 to 60 °C for BRH. This suggests that the adsorption of 2,4-D by GAC and BRH is endothermic, which it is attributed to the formation of new active sites or enlargement of pore size on the GAC or BRH surface and increased mobility of 2,4-D molecules at higher temperatures, thus resulting

in higher permeation within GAC or BRH (Amiri et al. 2016; Arshadi et al. 2016). In the case of MWCNTs, temperature is not an important parameter for elimination of 2,4-D from simulated wastewater. These findings are in accordance with those of Bahrami et al. (2017b), which found that an increase in temperature did not have a marked influence on the percentage removal of caffeine from wastewater by MWCNTs. Our findings show that the majority of 2,4-D (95%) was eliminated from simulated wastewater by MWCNTs at an initial concentration of 50 mg L^{-1} and a temperature of 20-40 °C.

The interactive effect of initial pollutant concentration and adsorbent dosage on 2,4-D removal efficiency by GAC, BRH and MWCNTs when the other three factors were kept fixed can be seen in Fig. 7. Thus, a sharp increment was found in the removal percentage of 2,4-D upon increasing the amount of adsorbent from 0.06 to 0.2 g for GAC and BRH and from 0.05 to 0.15 g for MWCNTs. This is because of the availability of more reactive adsorption sites upon increasing the quantity of adsorbents, which means that more 2,4-D molecules are adsorbed.

The residual plots of the CCD-RSM design for GAC, BRH and MWCNTs are presented in Figs. 8, 9, 10 and 11. These figures confirm the effectiveness and reliability of the CCD-RSM design as regards optimizing the removal of 2,4-D from simulated wastewater by varying operational parameters; this indicates that the least common squares suppositions are being established. The error histogram of adsorption capacities for BRH, GAC and MWCNTs (mg g^{-1}) is shown in Fig. 8. As can be seen, the error distribution of adsorption capacities for the three proposed adsorbents is not entirely normal and the curve is almost symmetrically bell-shaped, thus suggesting that the CCD-RSM satisfies the suppositions of normality. The internally standardized residuals were used to plot the normal probability chart (see Fig. 9), which is nearly linear, thus suggesting that the standardized residuals follow an essentially normal distribution. The internally standardized residuals curves for removal of 2,4-D by GAC,

BRH and MWCNTs in batch experiment mode are presented in Fig. 10. As can be seen, the standard residuals of the three adsorbents investigated fluctuate around the center line, with a highest observation order of ±3.5. The residuals versus fits for all three adsorbents are presented in Fig. 11, which shows a random scatter in the residuals and a constant variance for the original observations.

The relationship between various variables that affect the elimination of 2,4-D from wastewater and the adsorption efficiency of GAC, BRH and MWCNTs is non-linear in nature. As such, prediction of the optimum value for different parameters to maximize the adsorption efficiency of 2,4-D is difficult. However, CCD-RSM can be used for this purpose. In order to achieve an almost 99.99% adsorption efficiency of GAC, BRH and MWCNTs for 2,4-D, the optimum amounts of various variables were found to be 0.2 g adsorbent, 60 mg L^{-1} 2,4-D concentration, pH 2, a temperature of 46 °C and 68.59 min contact time for GAC; 0.2 g adsorbent, 60 mg L^{-1} 2,4-D concentration, pH 5.5, a temperature of 60 °C and 79.99 min contact time for BRH; and 0.15 g adsorbent, 50 mg L^{-1} 2,4-D concentration, pH 2, a temperature of 20 °C and 5 min contact time for MWCNTs (see Fig. 12). To assess the performance of CCD-RSM design in predicting the optimum values for several operational parameters, adsorption experiments were performed under the conditions proposed by CCD-RSM. The results obtained were in good agreement with the experimental data. Thus, the calculated adsorption efficiency predicted for GAC, BRH and MWCNTs using the CCD-RSM model was found to be 99.98%, 99.99% and 99.99%, respectively, whereas the experimental adsorption efficiency of GAC, BRH and MWCNTs was found to be 97.32%, 96.8% and 95.99%, respectively.

Mathematical isotherm models

The Langmuir, Freundlich, Langmuir-Freundlich and Redlich-Peterson equations were applied as isotherm models to fit the experimental data for 2,4-D removal using GAC, BRH and MWCNTs. These isotherm models correlate between 2,4-D concentration in solution and the

amount of 2,4-D adsorbed on the adsorbents at a constant temperature (Arshadi et al. 2014). The values obtained for the adsorption isotherm parameters are shown in Table 7, which clearly reveals that the Freundlich and Redlich–Peterson models exhibit a very good performance, with a higher R^2 and lower SEE. The Freundlich model is an empirical equation and supposes that the surface of GAC, BRH and MWCNTs is heterogeneous and has varying pores, which can be used for multilayer adsorption (Hameed et al. 2009; Arshadi et al. 2014). In contrast, the Redlich-Peterson model is an adaptation of the Freundlich and Langmuir isotherm models that is suitable for microporous adsorption (Bahrami et al. 2017a). In practice, two-parameter equations have received more attention due to their simplicity and high accuracy (Amiri et al. 2016). Accordingly, the Freundlich model has the highest R^2 and the lowest SEE compared to the other models. In the Freundlich model, k_F and n are the maximum adsorption capacity and the adsorption intensity, respectively, and are related to the affinity of GAC, BRH and MWCNTs for 2,4-D. Indeed, the values of $1/n$ in the range $0 < 1/n < 1$ display suitable adsorption isotherms, whereas $1/n > 1$ displays an unsuitable adsorption isotherm. The values of $1/n$ demonstrate that the adsorption of 2,4-D on GAC, BRH and MWCNTs is suitable. The values for k_F obtained using the Freundlich model (23.19, 19.41 and 14.72 for GAC, BRH and MWCNTs, respectively) suggest that the 2,4-D binding affinity follows the order GAC > BRH > MWCNTs. Similarly, the 2,4-D adsorption capacities for the adsorbents investigated follow the order GAC > BRH > MWCNTs. A comparison of the adsorption capacities for GAC, BRH and MWCNTs with those reported elsewhere for 2,4-D removal from simulated wastewater are tabulated in Table 8. These results show that the applied adsorbents perform similarly or even better to other adsorbents.

Drainage water sample

The adsorbents studied in this research were also used to remove 2,4-D from drainage water. Compared with the results obtained using simulated wastewater and GAC, BRH and

MWCNTs, the percentage removal of 2,4-D from drainage water increased to 100%, thus indicating the presence of co-existing cations and anions in drainage water with no effect on the 2,4-D adsorbance efficiency. These results show that GAC, BRH and MWCNTs are reliable and potentially useful for the removal of 2,4-D from agricultural drainage system.

Adsorption mechanism

In the case of GAC, a chemical reaction between the surface of the adsorbent and the hydroxyl groups in 2,4-D may occur. As a consequence, a covalent bond is established between 2,4-D and the surface of GAC due to the surface charge of the GAC, the speciation of 2,4-D and the degree of ionization. At pH 2, 2,4-D contains reactive sites which would be adsorbed onto the carbon surface. Moreover, the mobility of 2,4-D in the surface and subsurface of GAC is increased at acidic pH. Overall, the presence of oxygen-containing functional groups on the surface of GAC increases its hydrophilic character and the number of binding sites available for the removal of 2,4-D. However, the adsorption of 2,4-D by GAC is complex, thus indicating that several mechanisms, including dispersion forces, may be involved. In the case of BRH, powerful H-bonds between 2,4-D and phenolate or carboxylate functional groups on the surface of the adsorbent, as well as π-π interactions between them, are the predominant adsorption mechanisms. In the case of MWCNTs, polarization of π electrons, a dispersion effect between the π electrons of the MWCNTs and the aromatic phenolic ring, as well as electrostatic attractions, are the predominant adsorption mechanism.

Economic analysis of the adsorbents using the ROR method

To evaluate the performance of GAC, BRH and MWCNTs for removal of 2,4-D in wastewater treatment systems, an economic analysis based on the ROR method was conducted. A typical wastewater treatment system, including economic information for the three adsorbents studied from the Iranian market, is presented in Table 9. Based on the results shown in this table, annual

costs include installation costs, operating costs, maintenance costs, replacement costs and indirect costs. Accordingly, the ROR is calculated for each adsorbent when the present worth of a project equals zero (Remer and Nieto 1995). The ROR for each project can be written as:

$$NPW_{GAC} = -10000 - 8600\left(\frac{P}{A}, i\%, 8\right) + 12000\left(\frac{P}{A}, i\%, 8\right) + 950\left(\frac{P}{F}, i\%, 8\right) = 0 \quad (6)$$

$$NPW_{BRH} = -7231 - 6250\left(\frac{P}{A}, i\%, 8\right) + 9000\left(\frac{P}{A}, i\%, 8\right) + 686\left(\frac{P}{F}, i\%, 8\right) = 0 \quad (7)$$

$$NPW_{MWCNTs} = -100000 - 15000\left(\frac{P}{A}, i\%, 8\right) + 28000\left(\frac{P}{A}, i\%, 8\right) + 8500\left(\frac{P}{F}, i\%, 8\right) = 0 \quad (8)$$

Upon solving above equations, the ROR for GAC, BRH and MWCNTs was calculated to be 30%, 35% and 3%, respectively. Those projects using GAC and BRH as adsorbents are considered to be economical since their ROR is higher than 15%, whereas the project using MWCNTs is inviable since its ROR is lower than 15%. An extra investment analysis was subsequently used to determine the best project, as follows (see Table 9):

$$NPW_{GAC-BRH} = -2769 - 2350\left(\frac{P}{A}, i\%, 8\right) + 3000\left(\frac{P}{A}, i\%, 8\right) + 264\left(\frac{P}{F}, i\%, 8\right) = 0 \quad (9)$$

Upon solving above equation, the ROR was calculated to be 10.8%, which is lower than 15%. This extra investment analysis implies that the project using BRH as adsorbent is more economical than the project using GAC because the BRH project has the lowest initial investment. This economic analysis using a rate of return (ROR) method therefore indicates that BRH could serve as an eco-friendly, low-cost, versatile and high adsorption capacity alternative to GAC and MWCNTs for the removal of 2,4-D.

Conclusions

The performance of GAC, BRH and MWCNTs for the removal of 2,4-D from simulated wastewater and drainage water was studied. In addition, a CCD-RSM design was applied for modeling in which the adsorption efficiency of adsorbents is affected by multiple operational factors, including pH, temperature, contact time, adsorbent dose and initial herbicide concentration. The following results were obtained in this work.

(1) An increase in adsorbent dosage and temperature and a decrease in pH and initial 2,4-D concentration result in an increase in the adsorption efficiency of 2,4-D by GAC and BRH.

(2) The results imply that the temperature and contact time do not have a marked effect on the adsorption efficiency of 2,4-D by MWCNTs.

(3) The equilibrium time for MWCNTs, GAC and BRH was achieved at 5, 70 and 80 min, respectively, thus indicating a rapid uptake of 2,4-D by MWCNTs within the first 5 min.

(4) The maximum adsorption capacities followed the order GAC > BRH > MWCNTs.

(5) An optimal 2,4-D removal of 97.32% was achieved with GAC at pH 2, a contact time of 68.59 min, a temperature of 46 °C, an adsorbent dose of 0.2 g, and an initial 2,4-D concentration of 60 mg L^{-1}.

(6) Maximum 2,4-D removal (96.8%) by BRH was achieved at pH 5.5, a contact time of 79.99 min, a temperature of 60 °C, an adsorbent dose of 0.2 g, and an initial 2,4-D concentration of 60 mg L^{-1}.

(7) The maximum percentage removal of 2,4-D (95.99%) by MWCNTs was obtained at pH 2, a contact time of 5 min, a temperature 30 °C, an adsorbent dose of 0.15 g, and an initial 2,4-D concentration of 50 mg L^{-1}.

(8) The results confirm that the Freundlich isotherm model with the highest R^2 and the lowest SEE satisfactorily fitted the 2,4-D experimental data.

(9) The CC-RSM technique is a useful tool for minimizing the number of batch experiments and determining the optimum operational parameters with interaction effects.

(10) In view of the practical application of adsorbents, BRH could serve as an eco-friendly, low-cost, versatile and high adsorption capacity alternative to GAC and MWCNTs for the removal of 2,4-D.

Acknowledgements

AG is grateful for financial support from Santander Bank through the Research Intensification Program.

References

Abigail M, Chidambaram R, (2016) Rice husk as a low cost nanosorbent for 2,4-dichlorophenoxyaceticacid removal from aqueous solutions. Ecol Eng 92: 97-105.

Ahmad AL, Tan LS, Shukor SRA, (2008) Dimethoate and atrazine retention from aqueous solution by nanofiltration membranes. J Hazard Mater 151: 71–77.

Ahmaruzzaman M, Gupta VK, (2011) Rice husk and its ash as low-cost adsorbents in water and wastewater treatment. Ind Eng Chem Res 50: 13589-13613.

Aksu Z, Kabaskal E, (2004) Batch adsorption of 2,4-dichlorophenoxy-acetic acid (2,4-D) from aqueous solution by granular activated carbon. Sep Purif Technol 35: 223-240.

Aksu Z, Kabaskal E, (2005) Adsorption characteristics of 2,4-D from aqueous solution on powdered activated carbon. J Environ Sci Health part B 40: 545-570.

Al-Qodah Z, Shawabkah R, (2009) Production and characterization of granular activated carbon from activated sludge. Braz J Chem Eng 26: 127-136.

Amiri MJ, Abedi-Koupai J, Eslamian S, Arshadi M (2016) Adsorption of Pb(II) and Hg(II) ions from aqueous single metal solutions by using surfactant-modified ostrich bone waste. Desalin Water Treat 57: 16522-16539.

Anisuzzaman S, Joseph C, Taufiq-Yap Y, Krishnaiah D, Tay V (2015) Modification of commercial activated carbon for the removal of 2,4-dichlorophenol from simulated wastewater. J King Saud Univ Sci 27: 318-330.

Arasteh R, Masoumi M, Rashidi AM, Moradi L, Samimi V, Mostafavi ST (2010) Adsorption of 2-nitrophenol by multi-wall carbon nanotubes from aqueous solutions. Appl Surf Sci 256: 4447-4455.

Arshadi M, Amiri MJ, Mousavi S (2014) Kinetic, equilibrium and thermodynamic investigations of Ni(II), Cd(II), Cu(II) and Co(II) adsorption on barley straw ash. Water Resour Ind 6: 1-17.

Arshadi M, Mousavinia F, Amiri MJ, Faraji AR (2016) Adsorption of methyl orange and salicylic acid on a nano-transition metal composite: Kinetics, thermodynamic and electrochemical studies. J Colloid Interface Sci 483: 118-131.

Bahrami M, Amiri MJ, Koochaki S (2017a) Removal of caffeine from aqueous solution using multi-wall carbon nanotubes: kinetic, isotherm, and thermodynamics studies. Pollution. 3: 539-552.

Bahrami M, Amiri MJ, Mahmoudi MR, Koochaki S (2017b) Modeling caffeine adsorption by multi-walled carbon nanotubes using multiple polynomial regression with interaction effects. J Water Health 15: 526-535.

Bakouri HE, Morillo J, Usero J, Oussani A (2008) Potential use of organic waste substances as an ecological technique to reduce pesticide groundwater contamination. J Hydrol 353: 335-342.

Bazrafshan E, Kord Mostafapour F, Faridi H, Farzadkia M, Sargazi SH, Sohrabi A (2013) Removal of 2, 4-dichlorophenoxyacetic acid (2,4-D) from aqueous environments using single-walled carbon nanotubes. Health Scope 2: 39-46.

Boivin A, Amella S, Schiavon M, Van Genuchten MT (2005) 2,4-dichlorophenoxyacetic acid (2,4-D) sorption and degradation dynamics in three agricultural soils. Environ. Pollut 138: 92-99.

Chen B, Chen Z, Lv S (2011) A novel magnetic biochar efficiently sorbs organic pollutants and phosphate. Bioresour Technol 102: 716-723.

Dehghani M, Nasseri S, Karamimanesh M (2014) Removal of 2,4-dichlorophenolyxacetic acid (2,4-D) herbicide in the aqueous phase using modified granular activated carbon. J Environ Health Sci Eng 12:28.

Deokar SK, Mandavgane SA (2015) Rice husk ash for fast removal of 2,4-dichlorophenoxyacetic acid from aqueous solution. Adsorpt Sci Technol 33: 429-440.

de Rezende EIP, Peralta-Zamora PG, Abate G (2011) Sorption study of herbicides with the clay minerals vermiculite and montmorillonite. Quim Nova 34: 21-27.

Ding L, Lu X, Deng H, Zhang X (2012) Adsorptive removal of 2,4-dichlorophenoxyacetic acid (2,4-D) from aqueous solutions using MIEX resin. Ind Eng Chem Res 51: 11226-11235.

Ebrahimizadeh MA, Amiri MJ, Eslamian SS, Abedi-Koupai J, Khozaei M (2009) The effects of different water qualities and irrigation methods on soil chemical properties. Res J Environ Sci 3: 497-503.

Edvin Vasu A (2008) Surface modification of activated carbon for enhancement of Nickel (II) adsorption. E J Chem 5: 814-819.

Ehyaee M, Safa F, Shariati Sh (2017) Magnetic nanocomposite of multi-walled carbon nanotube as effective adsorbent for methyl violet removal from aqueous solutions: Response surface modeling and kinetic study. Korean J Chem Eng 34: 1051-1061.

Hallin IL, Douglas P, Doerr SH, Bryant R, Charbonneau C (2017) The potential of biochar to remove hydrophobic compounds from model sandy soils. Geoderma 285: 132-140.

Hameed BH, Salman JM, Ahmad A (2009) Adsorption isotherm and kinetic modeling of 2,4-D pesticide on activated carbon derived from date stones. J Hazard Mater 163: 121-126.

Han D, Jia W, Liang H (2010) Selective removal of 2,4-dichlorophenoxyacetic acid from water by molecularly-imprinted amino-functionalized silica gel sorbent. J Environ Sci 22: 237-241.

Humbert H, Gallard H, Suty H, Croue JP (2008) Natural organic matter (NOM) and pesticides removal using a combination of ion exchange resin and powdered activated carbon (PAC). Water Res 42: 1635-1643.

Iannazzo D, Pistone A, Ziccarelli I, Espro C, Galvagno S, Giofré SV, Romeo R, Cicero N, Bua GD, Lanza G, Legnani L, Chiacchio MA (2017) Removal of heavy metal ions from wastewaters using dendrimer-functionalized multi-walled carbon nanotubes. 24: 14735-14747.

Imagawa A, Seto R, Nagaosa Y (2000) Adsorption of chlorinated hydrocarbons from air and aqueous solutions by carbonized rice husk. Carbon 38: 623-641.

Jung BK, Hasan Z, Jhung SH (2013) Adsorptive removal of 2,4-dichlorophenoxyacetic acid (2,4-D) from water with a metal-organic framework. Chem Eng J 234: 99-105.

Kearns JP, Wellborn LS, Summers RS, Knappe DRU (2014) 2,4-D adsorption to biochars: effect of preparation conditions on equilibrium adsorption capacity and comparison with commercial activated carbon literature data. Water Res 62: 20-28.

Lehman JH, Terrones M, Mansfield E, Hurst KE, Meunier V (2011) Evaluating the characteristics of multiwall carbon nanotubes. Carbon 49: 2581-2602.

Li Q, Sun J, Ren T, Gue L, Yang Zh, Yang Q, Chen H (2017) Adsorption mechanism of 2,4-dichlorophenoxyacetic acid onto nitric acid modified activated carbon fiber. Environ Technol 7: 1-12.

Li X, Zhao H, Quan X, Chen Sh, Zhang Y, Yu H (2011) Adsorption of ionizable organic contaminants on multi-walled carbon nanotubes with different oxygen contents. . J Hazard Mater 186: 407-415.

Liang L, Zhang J, Feng P, Li C, Huang Y, Dong B, Li L, Guan X (2015) Occurrence of bisphenol A in surface and drinking waters and its physicochemical removal technologies. Front Environ Sci Eng 9: 16–38.

Mandal S, Sarkar B, Igalavithana AD, Ok YS, Yang X, Lombi E, Bolan N (2017) Mechanistic insights of 2,4-D sorption onto biochar: Influence of feedstock materials

and biochar properties. Bioresour Technol 246: 160-167.

Manna S, Saha P, Roy D, Sen R, Adhikari B (2016) Removal of 2,4-dichlorophenoxyacetic acid from aqueous medium using modified jute. J Taiwan Inst Chem Eng 67: 292-299.

Mohammad SG, Ahmed SM (2017) Preparation of environmentally friendly activated carbon for removal of pesticide from aqueous media. Int J Ind Chem 8: 121-132.

Mourabet M, El Rhilassi A, El Boujaady H, Bennani-Ziatni M, Taitai A (2017) Use of response surface methodology for optimization of fluoride adsorption in an aqueous solution by Brushite. Arabian J Chem 10: S3292–S3302.

Nethaji S, Sivasamy A (2017) Graphene oxide coated with porous iron oxide ribbons for 2, 4-dichlorophenoxyacetic acid (2,4-D) removal. Ecotox Environ Safe 138: 292-297.

Qu X, Alvarez PJJ, Li Q (2013) Applications of nanotechnology in water and wastewater treatment. Water Res 47: 3931-3946.

Remer D, Nieto A (1995) A compendium and comparison of 25 project evaluation techniques, part 1: Net present value and rate of return methods. Int J Prod Econ 42: 79-96.

Rostamian R, Heidarpour M, Mousavi SF, Afyuni M (2015) Preparation, characterization and sodium sorption capability of rice husk carbonaceous adsorbents. Fresen Environ Bull 24: 1649-1658.

Salmon JM, Hameed BH (2010) Adsorption of 2,4-dichlorophenoxyacetic acid and carbofuran pesticides onto granular activated carbon. Desalination 256: 129-135.

Salman JM, Njoku VO, Hameed BH (2011) Adsorption of pesticides from aqueous solution onto banana stalk activated carbon. Chem Eng J 174: 41-48.

Santacruz G, Bandala ER, Torres LG (2005) Chlorinated pesticides (2,4-D and DDT) biodegradation at high concentrations using immobilized Pseudomonas fluorescens. J Environ Sci Health part B 40: 571-583.

Saritha P, Aparna C, Himabindu V, Anjaneyulu Y (2007) Comparison of various advanced oxidation processes for the degradation of 4-chloro-2 nitrophenol. J Hazard Mater 149: 609–614.

Shirmardi M, Alavi N, Babaei A (2016) Removal of atrazine as an organic micropollutant from aqueous solutions: a comparative study. Process Saf Environ Prot 103: 23-35.

Srivastava VC, Mall ID, Mishra IM (2006) Characterization of mesoporous rice husk ash (RHA) and adsorption kinetics of metal ions from aqueous solution onto RHA. J Hazard Mater 134: 257-267.

United States Environmental Protection Agency (2015) “Notification per PRN 98-10 –Minor Label Updates; Change of Primary Brand Name to Amine 4 2,4-D Weed Killer” Rep. No. EPA-34704-120, Washington, DC. Available at: https://www3.epa.gov/pesticides/chem_search/ppls/034704-00120-20151106.pdf.

Wang Y, Liu R (2017) Comparison of characteristics of twenty-one types of biochar and their ability to remove multi-heavy metals and methylene blue in solution. Fuel Process Technol 160: 55-63.

Wang Y, Ma J, Zhu J, Ye N, Zhang X, Huang H (2016) Multi-walled carbon nanotubes with selected properties for dynamic filtration of pharmaceuticals and personal care products. Water Res 92: 104-112.

Zeng Z-w, Tian S-r, Liu Y-g, Tan X-f, Zeng G-m, Jiang L-h, Yin Z-h, Liu N, Liu S-b, Li J (2018) Comparative study of rice husk biochars for aqueous antibiotics removal. J Chem Technol Biotechnol 93: 1075-1084.

.

Captions

Table 1. Physical characteristics of the materials.

Table 2. Chemical structure and physicochemical properties of 2,4-dichlorophenoxyacetic acid.

Table 3. Experimental range of input parameters.

Table 4. Mathematical equations for the isotherm models.

Table 5. Characteristics of the drainage water.

Table 6. Selection of adsorbents to remove 2,4-D.

Table 7. Parameters for 2,4-D adsorption by the materials indicated.

Table 8. Comparison of 2,4-D adsorption capacities for various materials.

Table 9. Economic information for wastewater treatment systems using the materials indicated.

Figure 1. Photography and SEM images of samples: (A) BRH powder, (B) GAC granules, (C) MWCNTs powder, (D) BRH, (E) BRH after 2,4-D adsorption, (F) GAC, (G) GAC after 2,4-D adsorption, (H) MWCNTs, (I) MWCNTs after 2,4-D adsorption.

Figure 2. FTIR images of BRH, GAC and MWCNTs before (A) and after (B) 2,4-D adsorption.

Figure 3. Zeta potential of BRH, GAC and MWCNTs at various pH values.

Figure 4. Contour and surface plots of adsorption efficiency versus the effect of the reaction time and pH for 2,4-D removal using GAC (A), BRH (B) and MWCNTs (C).

Figure 5. Surface plots of interaction effects of reaction time and C_0 on adsorption of 2,4-D by GAC (A), BRH (B) and MWCNTs (C).

Figure 6. Contour plots of interaction effects of temperature and C_0 on adsorption of 2,4-D by GAC (A), BRH (B) and MWCNTs (C).

Figure 7. Contour and surface plots of interaction effects of C_0 and $C_s$on adsorption of 2,4-D by GAC (A), BRH (B) and MWCNTs (C).

Figure 8. Histogram of the residuals to optimize the removal of 2,4-D from simulated wastewater using GAC (A), BRH (B) and MWCNTs (C).

Figure 9. Normal probability plot of residuals to optimize the removal of 2,4-D from simulated wastewater using GAC (A), BRH (B) and MWCNTs (C).

Figure 10. Observation order for 2,4-D removal from simulated wastewater using GAC (A), BRH (B) and MWCNTs (C).

Figure 11. Residuals versus fits for 2,4-D removal from simulated wastewater using GAC (A), BRH (B) and MWCNTs (C).

Figure 12. Optimization response plot for the maximum adsorption of 2,4-D from simulated wastewater using GAC (A), BRH (B) and MWCNTs (C).

743

Table 1. Physical characteristics of the materials. 744

Adsorbent materials	**BRH**	**GAC**	**MWCNTs**
Diameter	0.5 - 3.5 µm	1 - 1.5 mm	10 - 20 nm
Length (µm)	-	-	30
Ash (wt.%)	18.5	14.6	< 1.5
Specific surface area ($m^2 g^{-1}$)	320	728	200
Average pore size (nm)	5.9	4.2	7.2
Pore volume ($cm^3 g^{-1}$)	0.431	0.748	0.348
Density ($g\ cm^{-3}$)	1.42	1.58	2.1

745

746

Table 2. Some of the physicochemical properties of 2,4-dichlorophenoxyacetic acid.

Characteristic	
Chemical formula	$C_8H_6Cl_2O_3$
Molecular weight ($g \cdot mol^{-1}$)	221.04
Solubility in water ($mg\ L^{-1}$)	900
Density ($g\ cm^{-3}$)	12
pKa	2.64
UV adsorption (nm)	283
Structure	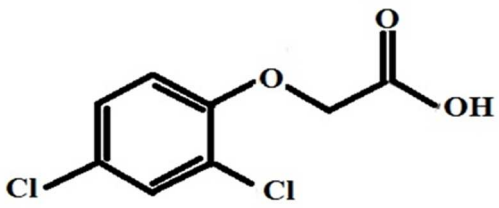

Table 3. Experimental range of input parameters.

Variables		Ranges and actual values of coded levels				
		-2.36	**-1**	**0**	**+1**	**+2.36**
C_0 (mg L^{-1})	**GAC**	100	300	450	600	800
	BRH	60	200	300	400	600
	MWCNTs	50	150	200	300	400
C_s (g)	**BRH**	0.06	0.1	0.125	0.15	0.2
	GAC	0.06	0.1	0.125	0.15	0.2
	MWCNTs	0.05	0.1	0.125	0.15	0.2
t (min)	**BRH**	15	45	68	90	120
	GAC	15	45	68	90	120
	MWCNTs	1	2	3	4	5
Initial pH	**BRH**	2	4	5.5	7	9
	GAC	2	4	5.5	7	9
	MWCNTs	2	4	5.5	7	9
T (ºC)	**BRH**	20	30	40	50	60
	GAC	20	30	40	50	60
	MWCNTs	20	30	40	50	60

765

Table 4. Mathematical equations for the isotherm models. 766

Model	Equation	Parameter and dimension
Langmuir	$q_e = \frac{k_L \cdot q_L C_e}{1 + k_L \cdot C_e}$	q_L (mg g^{-1}) k_L (L mg^{-1})
Freundlich	$q_e = k_F C_e^{1/n}$	k_F (mg g^{-1}) n: model exponent (–)
Langmuir-Freundlich	$q_e = \frac{q_{LF} \cdot (k_{LF} \cdot C_e)^{1/m}}{1 + (k_{LF} \cdot C_e)^{1/m}}$	k_{LF} (L mg^{-1}) m (–) (0 < n < 1)
Redlich-Peterson	$q_e = \frac{k_{RP} \cdot C_e}{1 + a_{RP} \cdot C_e^{\beta}}$	k_{RP} (L g^{-1}) a_{RP} (L mg^{-1}) β (–) (0 < β < 1)

767

768

Table 5. Characteristics of the drainage water.

	pH	Na^+	K^+	Mg^{2+}	Ca^{2+}	Cl^-	HCO_3^-	SO_4^{2-}	2,4-D
Amount	8.1	984*	11.8*	121.65*	160.5*	1328*	365*	827.5*	250**

*ppm, ** ppb

773

Table 6. Selection of adsorbents to remove 2,4-D. 774

number	adsorbent	number	adsorbent
1	Fish bone waste	8	Wheat ash
2	Ostrich bone ash	9	Oat ash
3	Synthesized hydroxyapatite (HA)	10	Barley ash
4	HA + CTABr	11	Starch
5	HA + CA	12	Cross-linked Starch
6	HA + CA+ NaOH	13	Shrimp shell
7	nZVI	14	Rice husk

775

776

Table 7. Parameters for 2,4-D adsorption by the materials indicated. 777

Models	**parameters**	**BRH**	**GAC**	**MWCNTs**
Langmuir	q_L	246	271	219
	k_L	2.28×10^{-4}	2.18×10^{-4}	4.08×10^{-4}
	R^2	0.998	0.999	0.997
	SEE	5.32	4.12	6.34
Freundlich	k_F	19.4	23.2	14.7
	1/n	0.34	0.54	0.61
	R^2	0.999	0.999	0.999
	SEE	0.05	0.07	0.09
Langmuir-Freundlich	q_{LF}	384.91	447	301.18
	k_{LF}	7.87×10^{-7}	6.03×10^{-7}	1.2×10^{-6}
	1/m	0.28	0.39	0.58
	R^2	0.69	0.52	0.75
	SEE	21.34	50.48	13.58
Redlich-Peterson	k_{RP}	0.48	0.50	0.51
	a_{RP}	-2×10^{-7}	-3.9×10^{-5}	0.024
	β	0.85	0.33	0.018
	R^2	0.998	0.999	0.999
	SEE	0.51	0.08	0.16

778

779

780

Table 8. Comparison of 2,4-D adsorption capacities for various materials. 781

Adsorbents	Adsorption capacity (mg g^{-1})	Reference
Granular activated carbon	181.82	Salmon and Hameed, 2010
Graphene oxide-Fe_3O_4 nanocomposites	67.26	Nethaji and Sivasamy, 2017
Cr-benzenedicarboxylate	556	Jung et al., 2013
Single-Walled Carbon Nanotubes	192.3	Bazrafshan et al., 2013
Banana stalk	196.33	Salman et al., 2011
Tea waste biochar	58.8	Mandal et al., 2017
Oak wood biochar	26.66	Mandal et al., 2017
Bamboo biochar	28.92	Mandal et al., 2017
MWCNTs	218.74	This work
GAC	271.05	This work
BRH	246.31	This work

782

783

Table 9. Economic information for wastewater treatment systems using the materials indicated.

Incomes and costs	GAC	BRH	MWCNTs	GAC-BRH
Initial investment ($)	10000	7231	100000	2769
Annual Cost ($)	8600	6250	15000	2350
Annual Incomes ($)	12000	9000	28000	3000
Salvage Value ($)	950	686	8500	264
Useful Life (year)	8	8	8	8
MARR	15	15	15	15

789

790

792

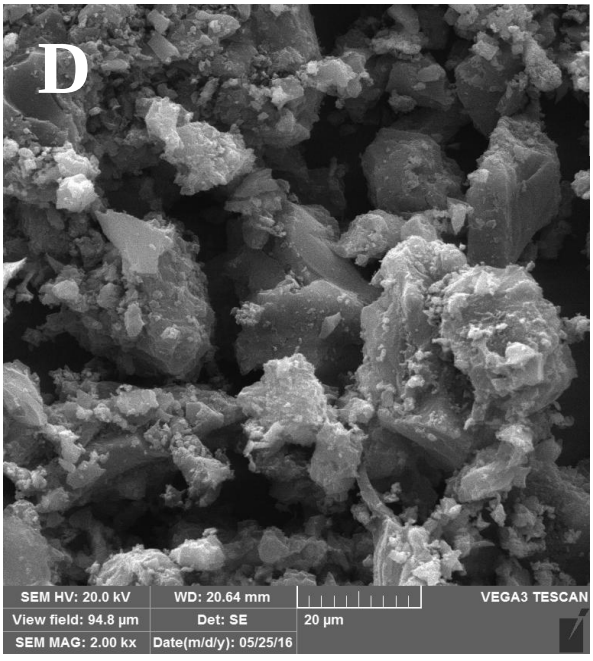

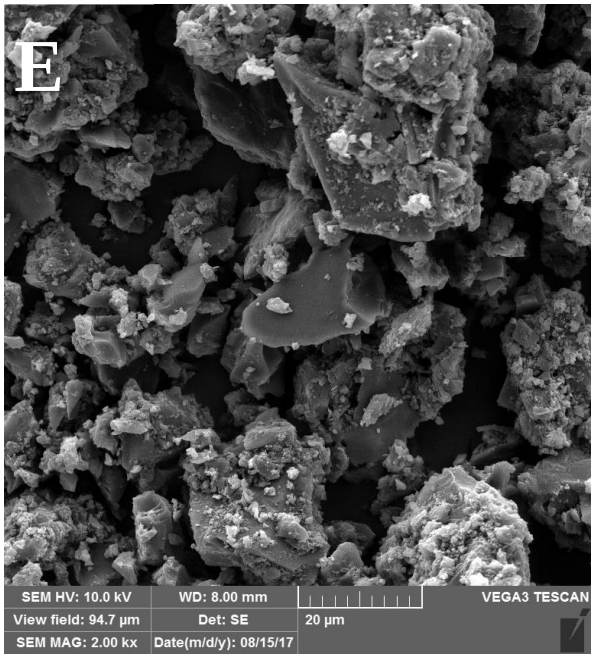

793

794

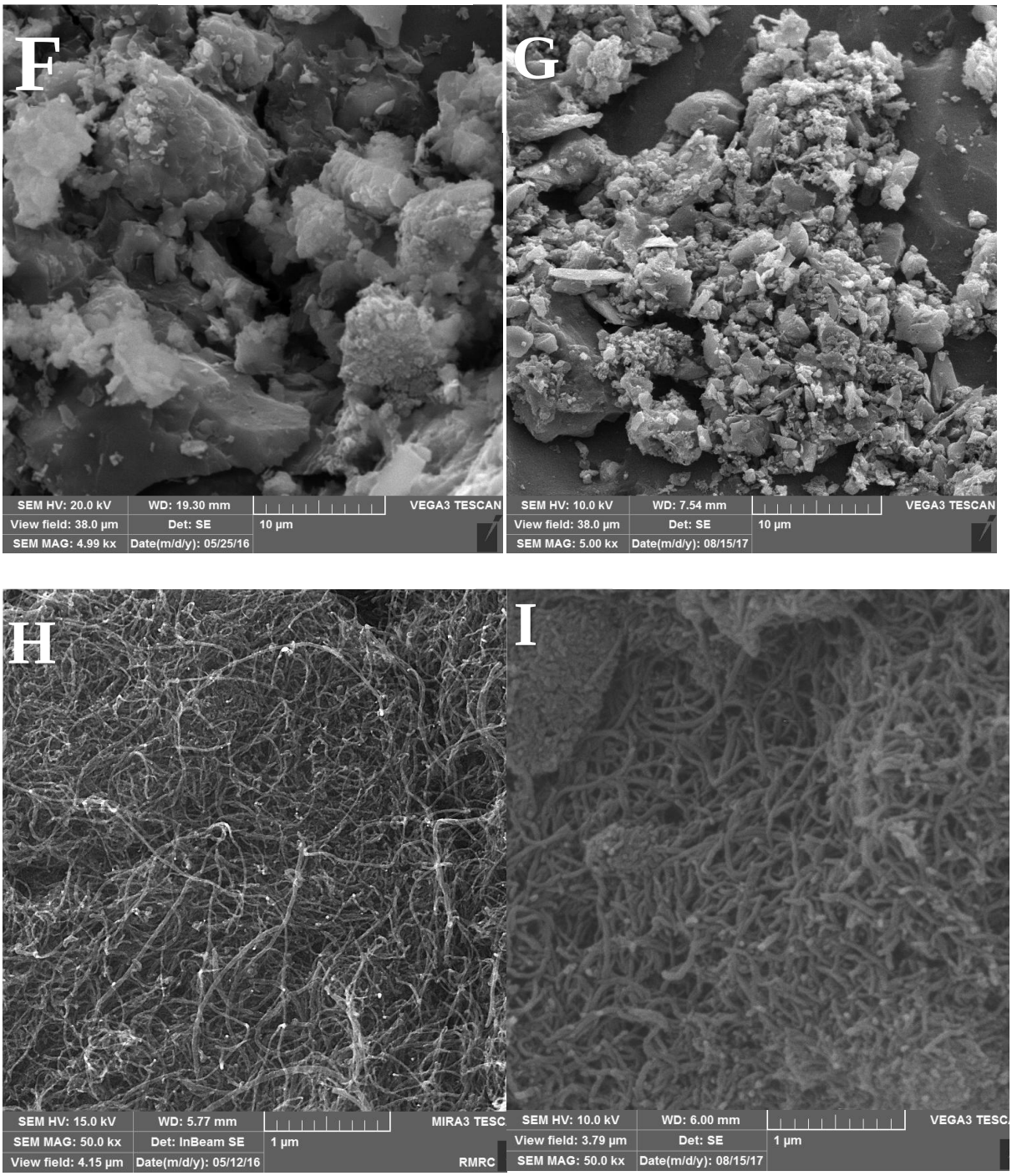

Figure 1. Photography and SEM images of samples: (A) BRH powder, (B) GAC granules, (C) MWCNTs powder, (D) BRH, (E) BRH after 2,4-D adsorption, (F) GAC, (G) GAC after 2,4-D adsorption, (H) MWCNTs, (I) MWCNTs after 2,4-D adsorption.

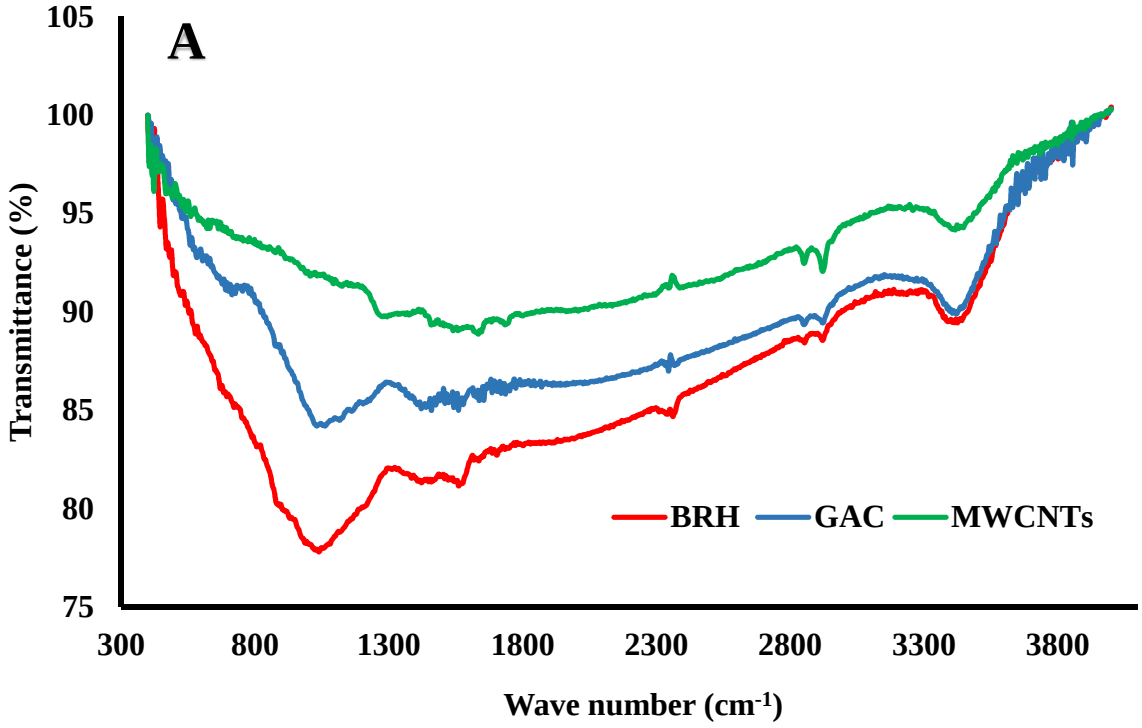

800

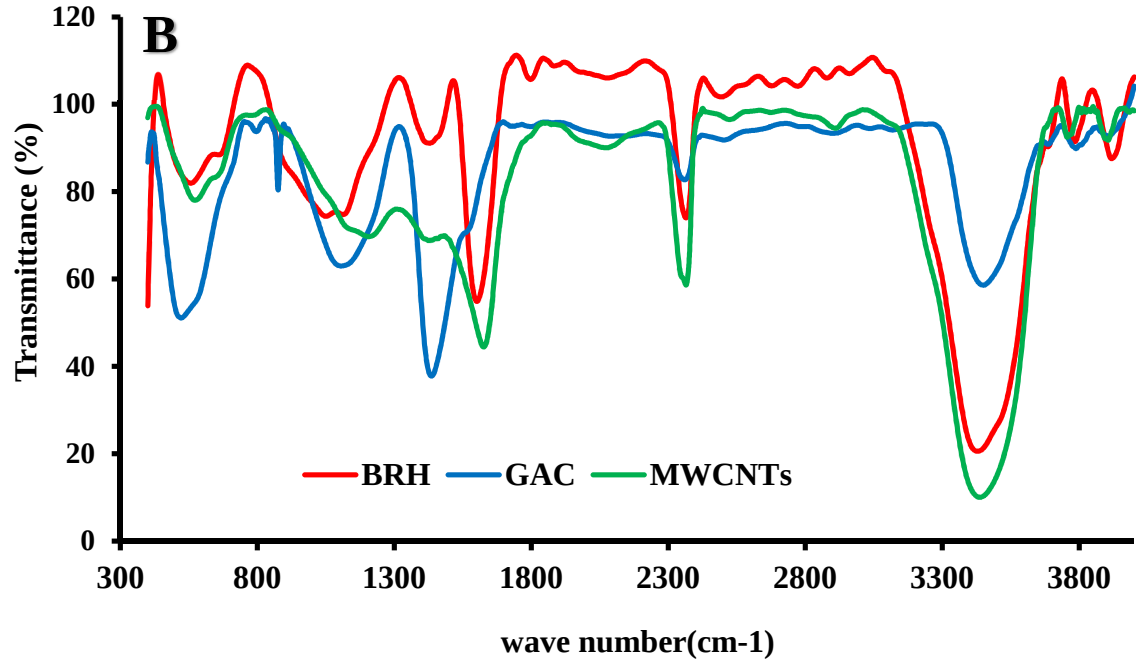

801

Figure 2. FTIR images of BRH, GAC and MWCNTs before (A) and after (B) 2,4-D adsorption. 802 803

804

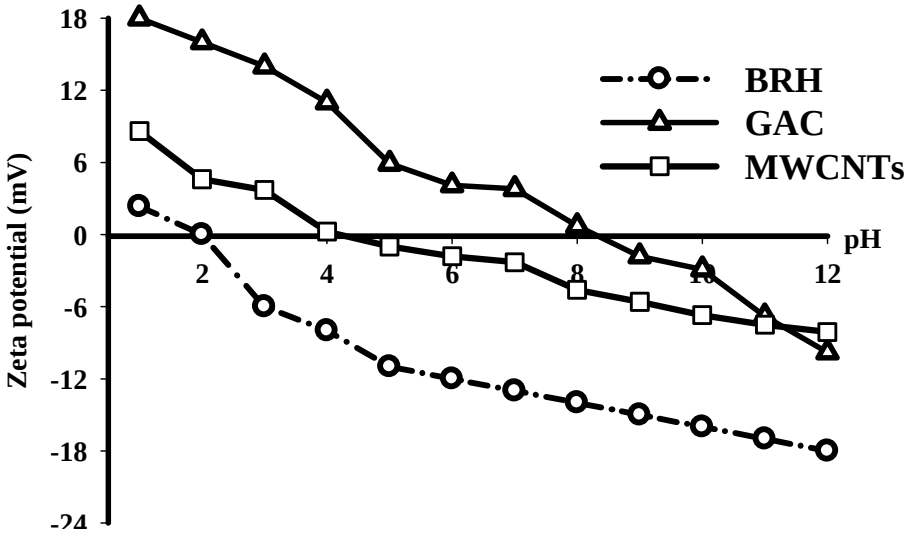

Figure 3. Zeta potential of BRH, GAC and MWCNTs at various pH values.

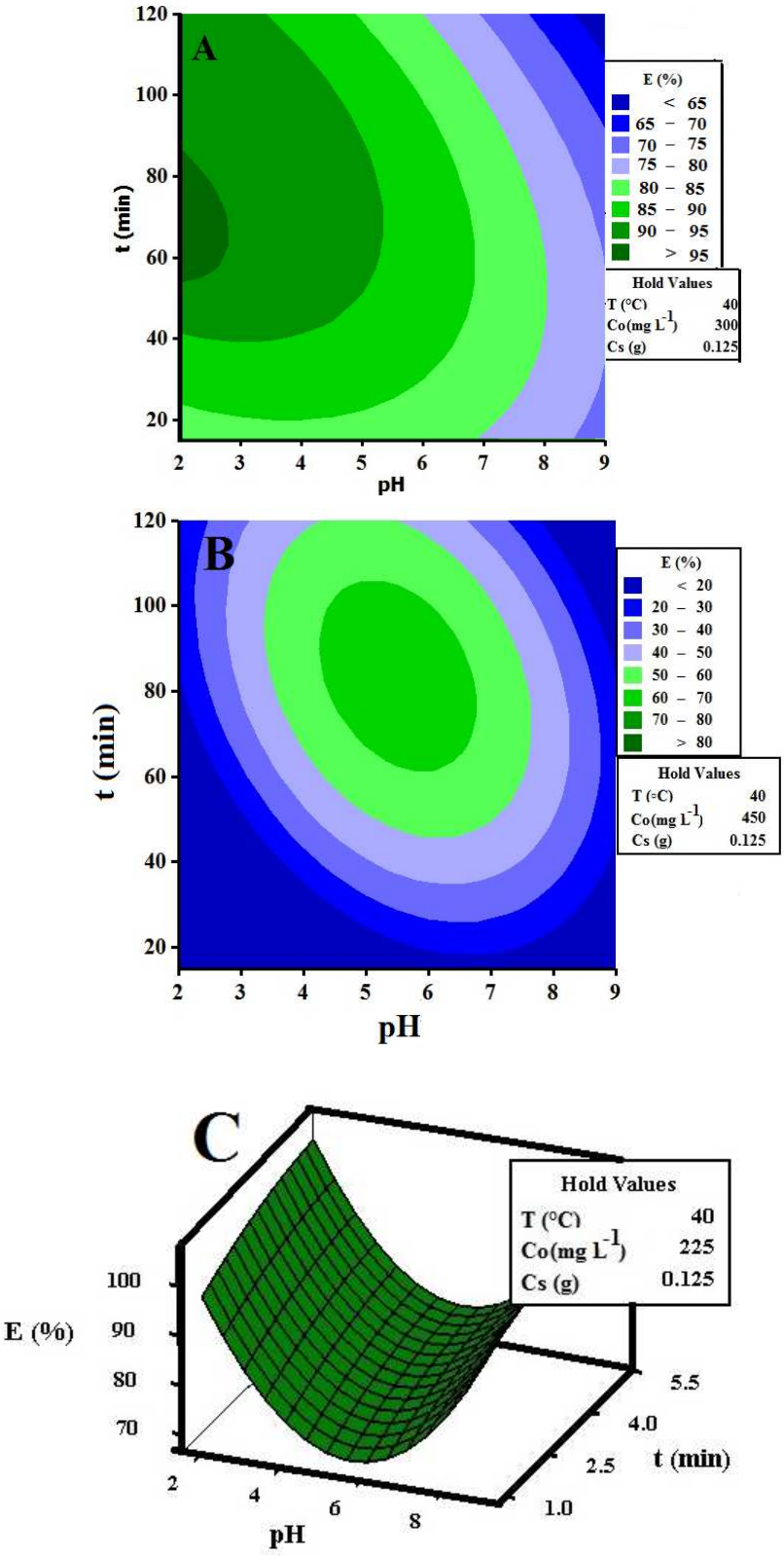

Figure 4. Contour and surface plots of adsorption efficiency versus the effect of the reaction time and pH for 2,4-D removal using GAC (A), BRH (B) and MWCNTs (C).

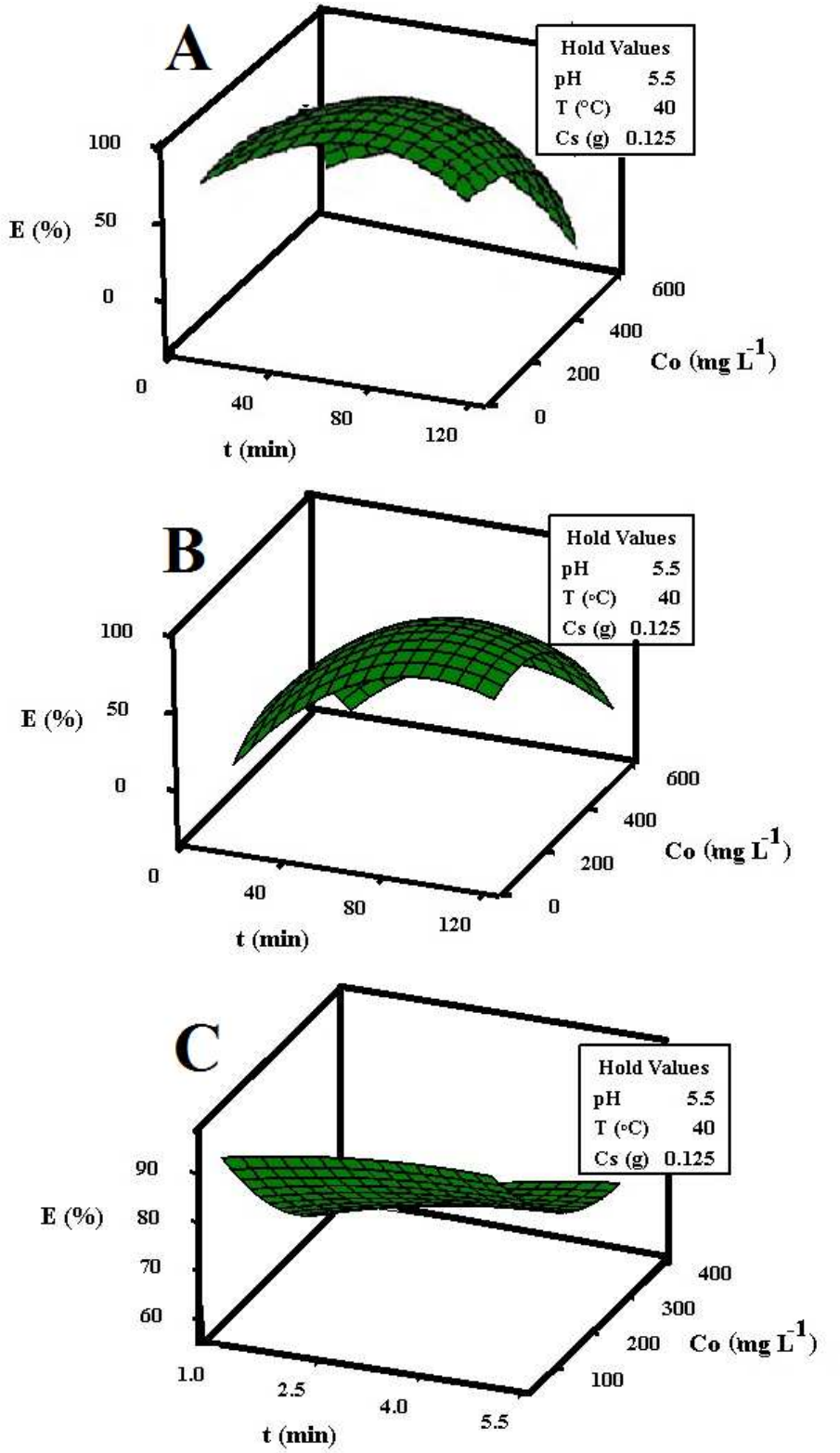

Figure 5. Surface plots of interaction effects of reaction time and C_0 on adsorption of 2,4-D by GAC (A), BRH (B) and MWCNTs (C).

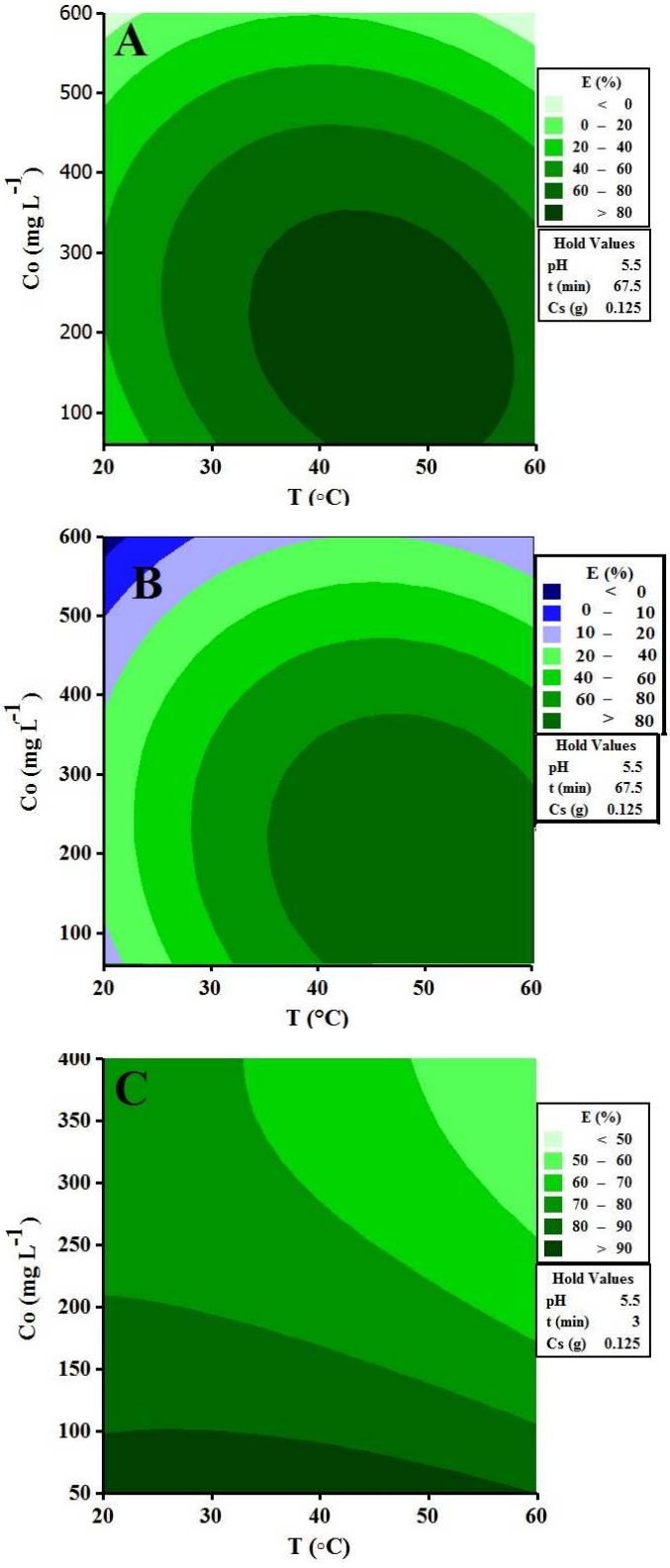

Figure 6. Contour plots of interaction effects of temperature and C_0 on adsorption of 2,4-D by GAC (A), BRH (B) and MWCNTs (C).

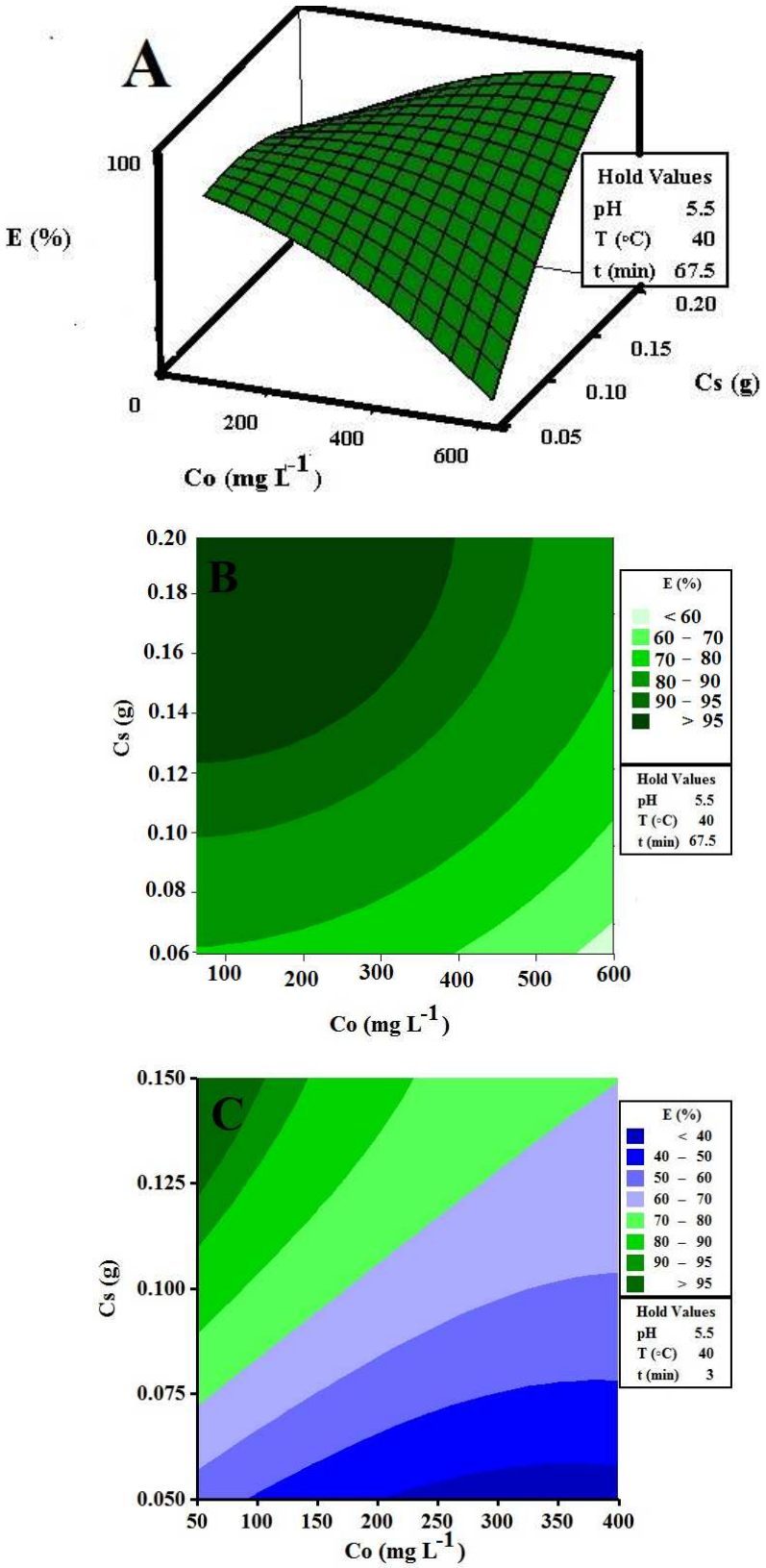

Figure 7. Contour and surface plots of interaction effects of C_0 and $C_s$on adsorption of 2,4-D by GAC (A), BRH (B) and MWCNTs (C).

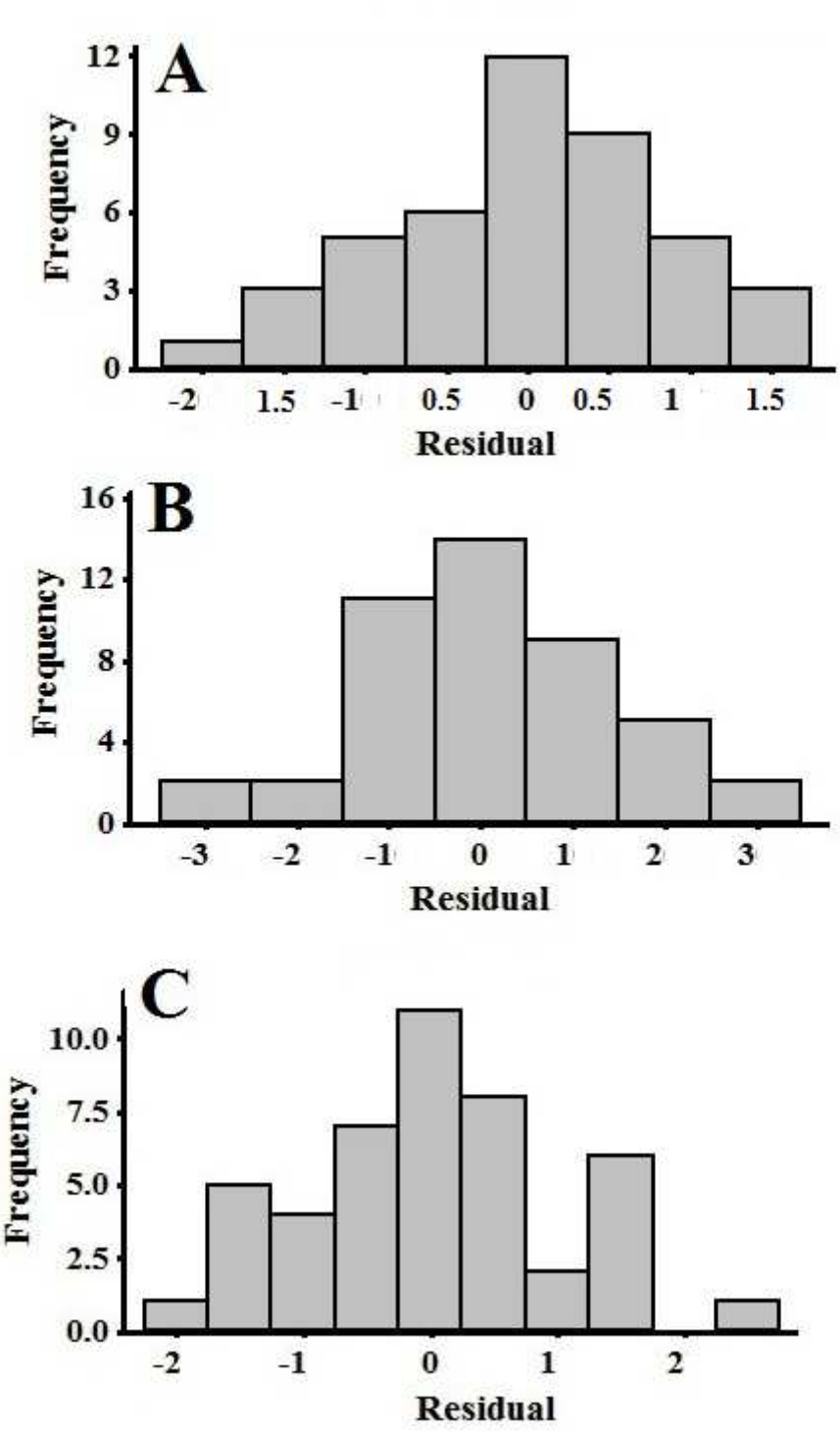

923

Figure 8. Histogram of the residuals to optimize the removal of 2,4-D from simulated wastewater using GAC (A), BRH (B) and MWCNTs (C). 924 925

926

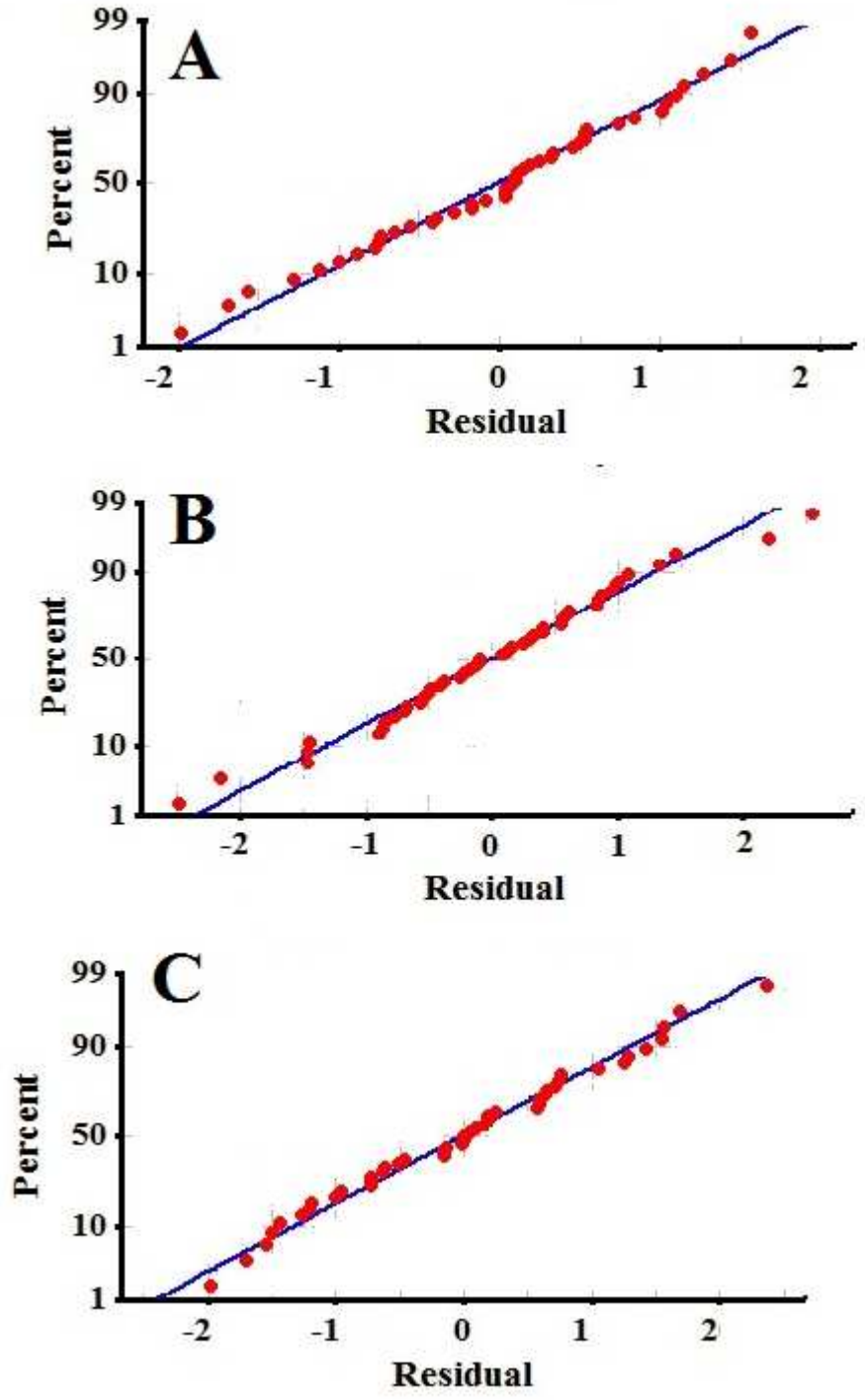

Figure 9. Normal probability plot of residuals to optimize the removal of 2,4-D from simulated wastewater using GAC (A), BRH (B) and MWCNTs (C).

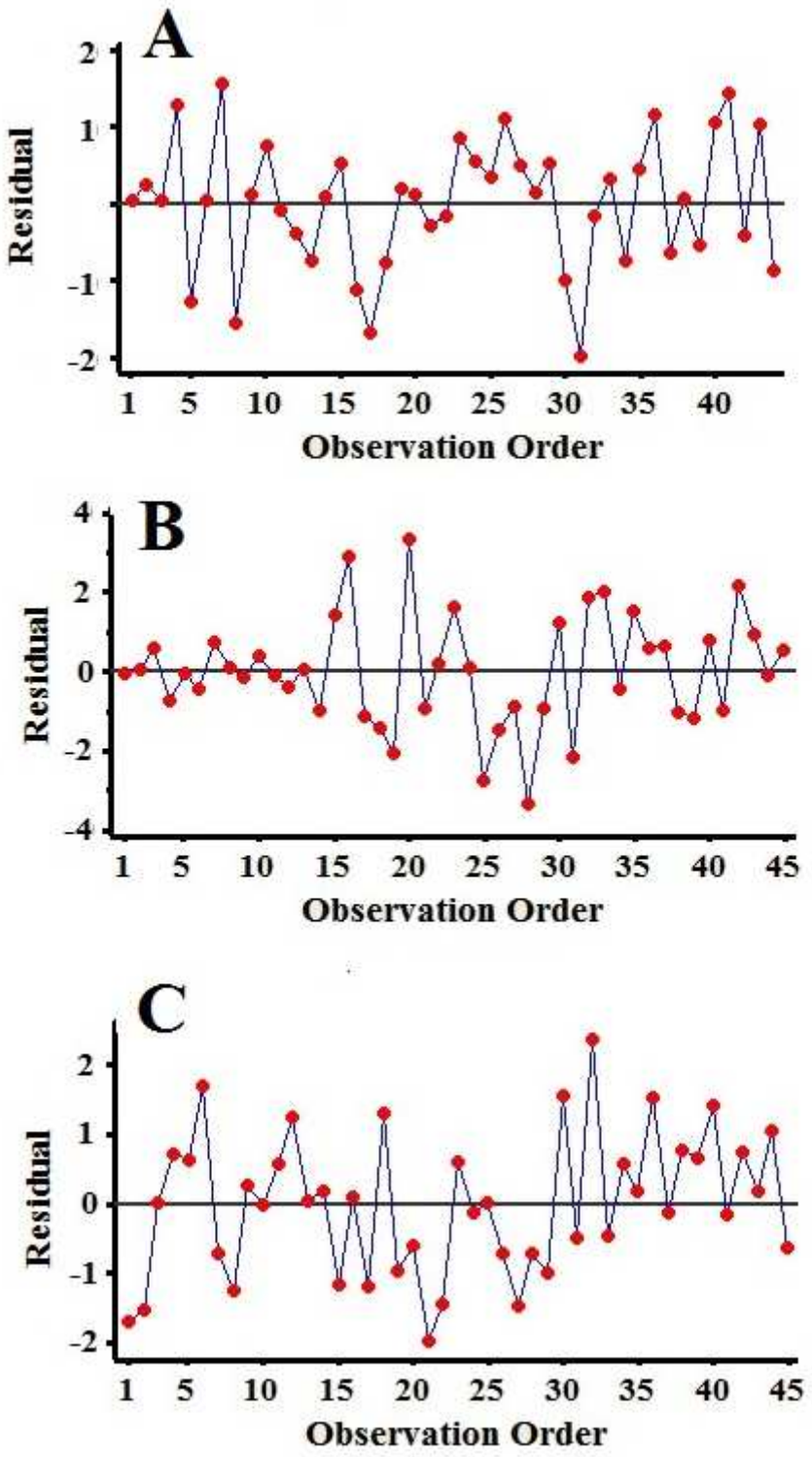

Figure 10. Observation order for 2,4-D removal from simulated wastewater using GAC (A), BRH (B) and MWCNTs (C).

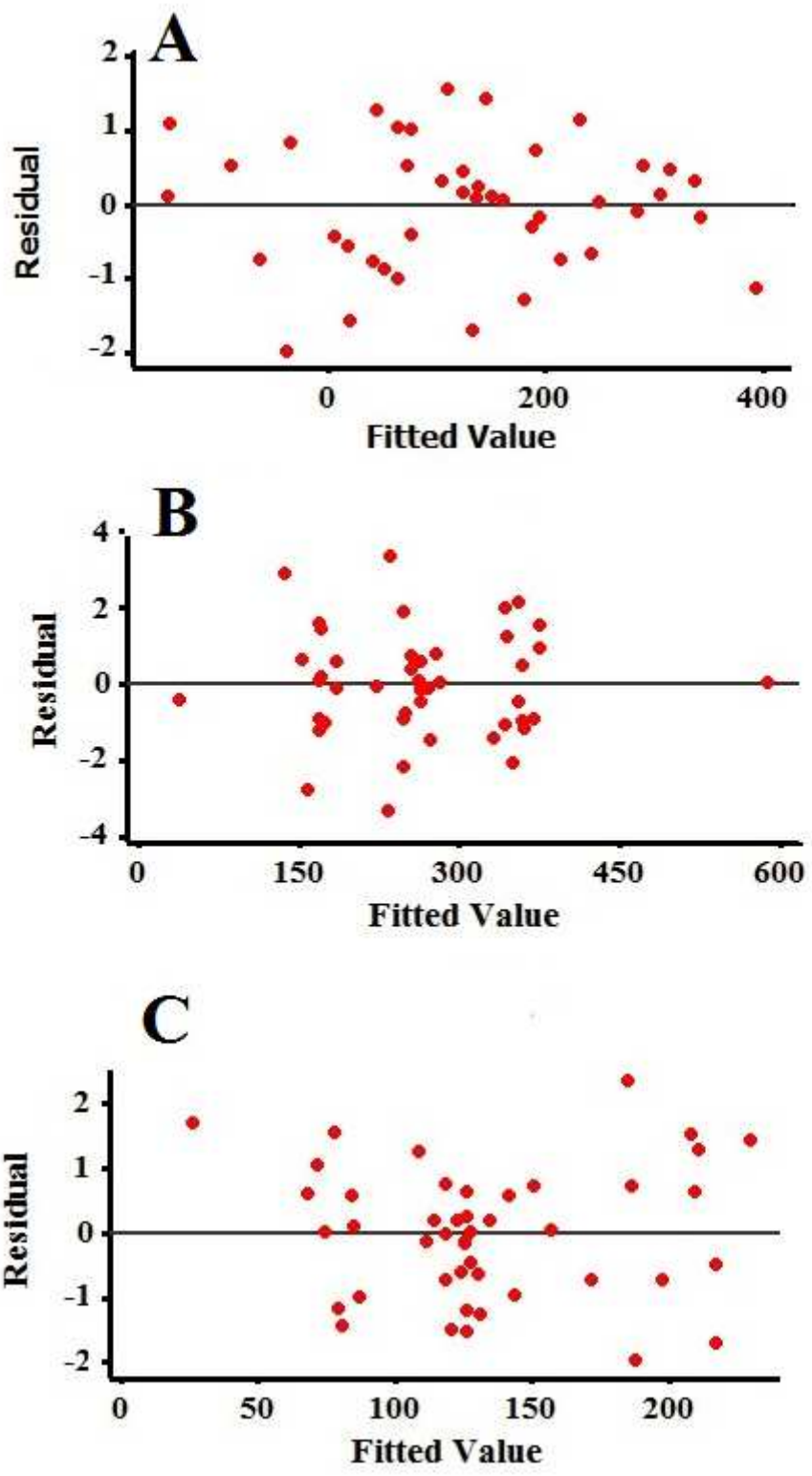

Figure 11. Residuals versus fits for 2,4-D removal from simulated wastewater using GAC (A), BRH (B) and MWCNTs (C).

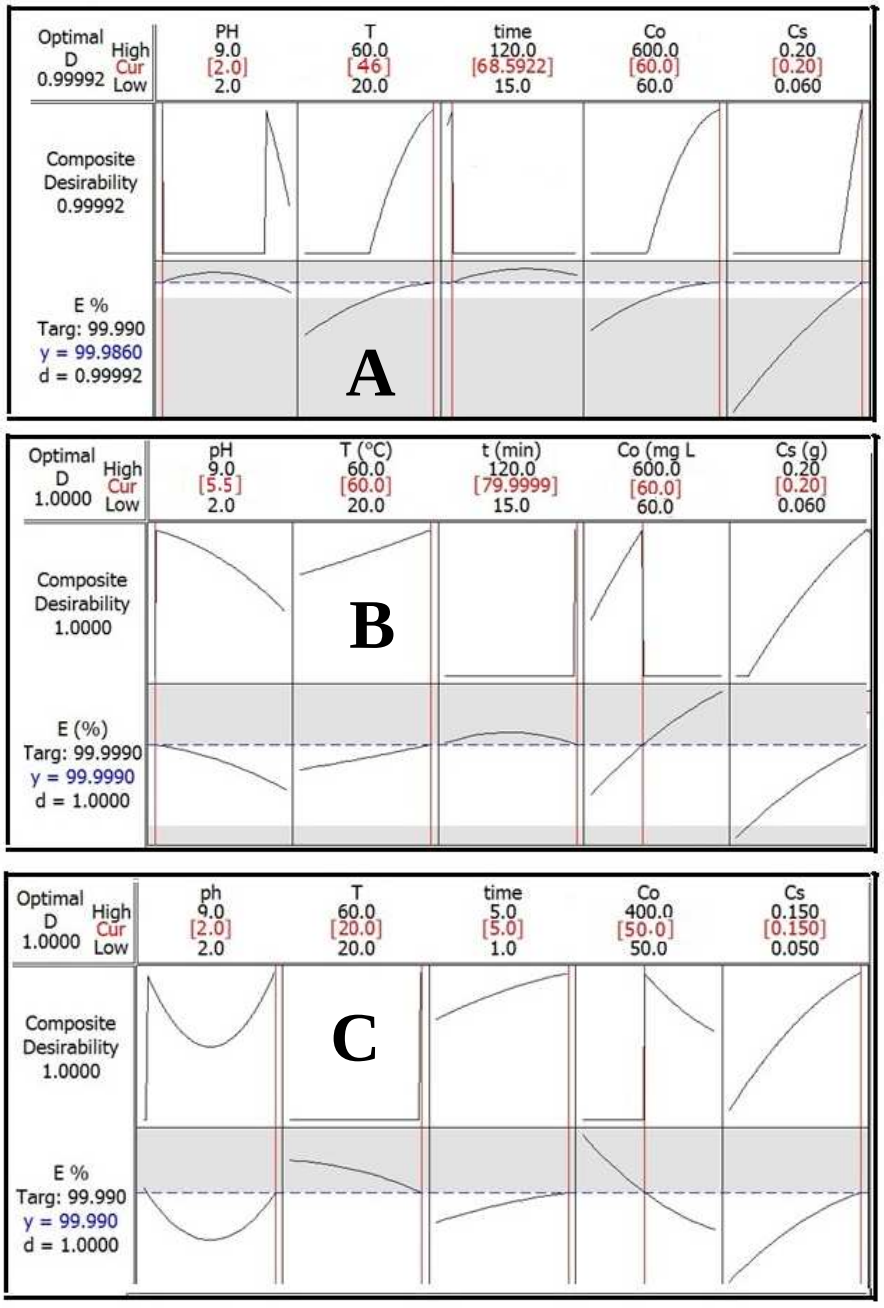

Figure 12. Optimization response plot for the maximum adsorption of 2,4-D from simulated wastewater using GAC (A), BRH (B) and MWCNTs (C).